

Supporting Information

Engineering a Highly Regioselective Fungal Peroxygenase for the Synthesis of Hydroxy Fatty Acids

*P. Gomez de Santos, A. González-Benjumea, A. Fernandez-Garcia, C. Aranda, Y. Wu, A. But, P. Molina-Espeja, D. M. Maté, D. Gonzalez-Perez, W. Zhang, J. Kiebist, K. Scheibner, M. Hofrichter, K. Świderek, V. Moliner, J. Sanz-Aparicio, F. Hollmann, A. Gutiérrez, M. Alcalde**

Table of contents:

Experimental Section	3
Table S1	11
Table S2	12
Table S3	14
Table S4	15
Table S5	17
Table S6	18
Table S7	20
Table S8	21
Figure S1	22
Figure S2	23
Figure S3	24
Figure S4	25
Figure S5	26
Figure S6	27
Figure S7	28
Figure S8	29
Figure S9	30
Figure S10	31
Figure S11	32
Figure S12	33
Figure S13	34
Figure S14	35
Figure S15	36
Figure S16	37
Figure S17	38
Figure S18	39
Figure S19	40
Figure S20	41
Figure S21	42
Figure S22	43
Figure S23	44

Experimental Section

Strains and chemicals

The *P. pastoris* expression vector (pPICZ-B), the *P. pastoris* strain X-33 and the antibiotic zeocin were purchased from Invitrogen (USA). The *Escherichia coli* strain XL2-Blue competent cells were obtained from Agilent Technologies (USA) and the protease-deficient *Saccharomyces cerevisiae* strain BJ5465 from LGCPromochem (Barcelona, Spain). Restriction endonucleases *EcoRI*, *XbaI*, *PmeI*, *BamHI* and *XhoI*, the DNA Ligation Kit and the Antarctic phosphatase were purchased from New England Biolabs (USA). iProof High-Fidelity DNA Polymerase was purchased from Bio-Rad (USA). Oligonucleotide primers were acquired from Integrated DNA Technologies (USA). NucleoSpin plasmid kit and NucleoSpin Gel and PCR Clean-up kit were purchased from Macherey Nagel (Germany). ABTS (2,2'-azino-bis(3-ethylbenzothiazoline-6-sulfonic acid)) was purchased from Panreac AppliChem (Germany), DMP (2,6-dimethoxyphenol), naphthalene and NBD (5-nitro-1,3-benzodioxole) from TCI Europe (Switzerland) and veratryl alcohol, propranolol hydrochloride, Purpald®, Fast Red (Fast Red TR salt hemi(zinc chloride) salt) benzyl alcohol, lauric (C₁₂), myristic (C₁₄), palmitic (C₁₆), stearic (C₁₈), palmitoleic (C_{16:1}) and oleic (C_{18:1}) acids, fatty acid methyl esters Me-C₁₆, Me-C₁₈, Me-C_{16:1}, Me-C_{18:1} and tetradecane were purchased from Merck Life Science (USA). All chemicals and media components were of the highest purity available.

Synthesis of 12-methoxylauric acid

12-methoxylauric acid (MLA) was synthesized as described elsewhere with minor modifications.^[1] 27.60 mmol KOH were added to 16 mL cooled dry MeOH and the solution was stirred for 1 h. Then a solution of 12-bromodecanoic acid (9.20 mmol) in 15 mL anhydrous MeOH was added using a syringe. The reaction mixture was heated to reflux and stirred for 16 h. After cooling to room temperature, MeOH was evaporated under vacuum, and the crude mixture reconstituted with 50 mL 1N HCl and 10 mL diethyl ether. The crude product was extracted using diethyl ether (4x60 mL), the combined layers were washed with 50:50 H₂O/water (60 mL) and dried over MgSO₄, and the solvent was evaporated under vacuum. MLA was purified by silica gel chromatography using a hexane/acetic acid/ethyl acetate gradient (99.8:0.2:0 to 98:1:1).

Yield: 1.61 g, 76% (white solid). ¹H NMR (400 MHz, CDCl₃): δ 3.37 (t, 2H, OCH₂), 3.34 (s, 3H, OCH₃), 2.34 (t, 2H, CH₂CO), 1.64 (2H, CH₂), 1.56 (dt, 2H, CH₂), 1.28 (14H, CH₂). ¹³C NMR (500 MHz, CDCl₃): δ 179.5, 34.0, 24.7, 29.2, 29.4, 29.4, 29.0, 29.6, 29.4, 26.1, 29.5, 73.0, 58.5.

Synthesis of methyl S-MTPA-13-hydroxymyristate

13-hydroxymyristic acid (15 mg, 61.4 μmol) obtained by Fett_{pic} was dissolved in methanol (1 ml). This solution was methylated with a solution of trimethylsilyldiazomethane in diethyl ether (60 μl, 120 μmol) at r.t. for 1 h. The reaction was dried in a rotary evaporator and the crude was purified by column chromatography in silica gel using EtOAc-hexane (10:1 → 5:1) as mobile phase obtaining methyl 13-hydroxymyristate as a colorless syrup (11.9 mg, 46.0 μmol).

Methyl 13-hydroxymyristate was dissolved in dry dichloromethane DCM (1 ml) and DMAP (7.3 mg, 59.8 μmol) and *R*-MTPA chloride (52 μl, 0.28 mmol) were added. The

mixture was stirred at r.t. and monitored by TLC until complete reaction. Finally, the *S*-MTPA ester was purified by column chromatography in silica gel using EtOAc-hexane (20:1 → 10:1) as mobile phase. Yield: 19.6 mg, 63% from myristic acid. ¹H-NMR (400 MHz, CDCl₃): δ 7.54-7.52 (m, 2H, Ph), 7.41-7.38 (m, 3H, Ph), 5.13 (sext, 1H, *J* = 6.3 Hz, H-13), 3.66 (s, 3H, Me), 3.57 (m, OMe (*R*)), 3.55 (m, 3H, OMe (*S*)), 2.30 (t, 2H, *J* = 7.5 Hz, H-2), 1.72-1.51 (m, 6H, H-3, H-4, H-12), 1.34-1.24 (m, 17H, H-5 to H-11, H-14). ¹³C-NMR (125 MHz, CDCl₃): δ 174.5, 166.3, 132.6, 129.6, 128.5, 127.5, 74.4, 55.5, 51.6, 35.8, 34.3, 29.7, 29.6, 29.5, 29.4, 29.3, 29.2, 25.5, 25.1, 19.6. ¹⁹F-NMR (500 MHz, CDCl₃): δ -71.44 (*S*), -71.49 (*R*).

Synthesis of methyl *R*-MTPA-13-hydroxymyristate

Methyl *R*-MTPA-13-hydroxymyristate was synthesized followed the procedure described above but using *S*-MTPA chloride as chiral derivatizing agent. Yield: 21.4 mg, 69% from myristic acid.

Library creation, microplate expression and screening

Saturation mutagenesis in position Ala 77: PCR reactions were performed in a final volume of 50 μl containing 3% v/v DMSO, 0.5 μM direct primer, 0.5 μM reverse primer, 1 mM dNTPs (0.25 mM each), 0.02 U/μL of iProof DNA polymerase (Bio-Rad), and 0.2 ng/μL pJRoC30-PaDa-I. For A77 saturation mutagenesis, the thermal cycler conditions set were 98°C for 30 s (1 cycle), 98°C 10 s, 47°C for 25 s, 72°C for 25 seg (28 cycles) and 72°C for 10 min (1 cycle) for RMLN/REV-77 (5'-caaggtgggcccgcataatgtnngaagattgcggttgattg-3') or 98°C for 30 s (1 cycle), 98°C 10 s, 52°C for 25 s, 72°C for 45 seg (28 cycles) and 72°C for 10 min (1 cycle) for DIR-77 (5'-caatcaagccgcaatcttcnsacatatgcccaccttg-3')/RMLC (saturation code: N=A/C/G/T, S=C/G).

Site-directed mutagenesis (SDM), SoLo-A77L variant: SoLo variant was subjected to SDM in order to obtain the variant with A77L mutation. PCR reactions for mutation of A77L were carried out with the primers A77L F (5'-caatttcgacaatcaagccgcaatctttgacatatgcccaccttgaggacggca-3') and A77L R (5'-tgccgtccacaaggtgggcccgcataatgtcaagaagattgcggttgattgaaattg-3'); mutated bases are underlined. The PCR reaction mixtures contained: 1) 50 μL final volume, DMSO (3%), RMLN (0.5 μM), A77L F (0.5 μM), dNTPs (1 mM, 0.25 mM each), high-fidelity DNA polymerase iProof (0.02 U/mL), and the template SoLo (10 ng), and 2) 50 μL final volume, DMSO (3%), RMLN (0.5 μM), A77L R (0.5 μM), dNTPs (1 mM, 0.25 mM each), iProof (0.02 U/mL), and the template SoLo (10 ng). PCR reactions were carried out on a gradient thermocycler using the following parameters: 98°C for 30 s (1 cycle); 98°C for 10 s, 48°C for 30 s, and 72°C for 30 s (28 cycles); and 72°C for 10 min (1 cycle).

All PCR products were loaded onto a preparative agarose gel and purified with the NucleoSpin Gel and PCR Clean-up kit. The recovered DNA fragments were cloned under the control of the GAL1 promoter of the pJRoC30 expression shuttle vector, with the use of BamHI and XhoI to linearize the plasmid and to remove the parent gene. The linearized vector was loaded onto a preparative agarose gel and purified with the NucleoSpin Gel and PCR Clean-up kit. The PCR products (200 ng each) were mixed with the linearized plasmid (100 ng) and transformed into *S. cerevisiae* for *in vivo* gene reassembly and cloning by IVOE.^[2]

The selective expression medium (SEM) contained filtered yeast nitrogen base (100 mL, 6.7%), filtered yeast synthetic drop-out medium supplement without uracil (100 mL, 19.2 g/L), filtered KH_2PO_4 buffer (pH 6.0, 67 mL, 1 M), filtered galactose (111 mL, 20%), filtered MgSO_4 (22 mL, 0.1 M), absolute ethanol (31.6 mL), filtered chloramphenicol (1 mL, 25 g/L), and $d\text{dH}_2\text{O}$ (to 1000 mL). Individual clones were picked and inoculated in sterile 96-well plates (Greiner Bio-One, GmbH, Germany), referred to as master plates, containing 200 mL of SEM per well. In each plate, column number 6 was inoculated with the parent type, and one well (H1-control) was inoculated with *S. cerevisiae* transformed with pJRoc30-MtL plasmid (laccase without activity). Plates were sealed with parafilm to prevent evaporation and incubated at 30 °C, 220 RPM and 80% relative humidity in a humidity shaker (Minitron, Infors, Switzerland) for five days. The master plates were centrifuged (Eppendorf 5810R centrifuge, Germany) for 10 min at 2,500g and 4°C. 20 μL of the supernatants were transferred from the master plates to two replica plates using a liquid handler robotic station (Freedom Evo, Tecan, Switzerland). The reaction mixtures for this high-throughput screening (HTS) with the substrates were added to each replica plate with the help of a pipetting robot (Multidrop, Thermo Fisher Scientific). The reaction mixture for ABTS screening contained 100 mM sodium citrate-phosphate pH 4.0 with 0.3 mM ABTS and 2 mM H_2O_2 , and was measured in endpoint mode at 418 nm in a plate reader (Spectramax Plus, Molecular Devices). The reaction mixture for NBD screening was composed of 100 mM potassium phosphate buffer pH 7.0 with 1 mM NBD, 15% (v/v) acetonitrile and 1 mM H_2O_2 , and was measured in endpoint mode at 425 nm. The reaction mixture for propranolol screening contained 50 mM phosphate buffer pH 7.0 with 5 mM propranolol and 2 mM H_2O_2 , and was measured in endpoint mode at 530 nm. The reaction mixture for naphthalene was composed of 100 mM potassium phosphate buffer pH 7.0, 0.5 mM naphthalene, 10% (v/v) acetonitrile and 1 mM H_2O_2 ; the plates were stirred briefly and the initial absorptions at 510 nm were recorded in the plate reader; after a reaction time of 10 min, Fast Red was added to each well (20 μL , final concentration of 0.5 mM) and the plates were incubated at room temperature until a red (naphthalene-Fast Red) colour appeared, moment at which the absorption at 510 nm was measured again. For MLA screening, aliquots of the supernatants (70 μL) were transferred from the master plates to the replica plates with the aid of the liquid handler. 80 μL of the reaction mixture were added to the replica plates with the help of a pipetting robot (Multidrop Combi Reagent Dispenser, Thermo Scientific, MA, USA). Reaction mixture contained 100 mM potassium phosphate buffer pH 7.0, 2 mM MLA (dissolved in 100% acetonitrile) and 2 mM H_2O_2 , with a final concentration of acetonitrile of 12.5%. Replica plates were incubated at room temperature for 60 min and afterwards, the amount of formaldehyde formed in each well due to terminal hydroxylation of MLA was determined by Purpald® assay. 50 μL of Purpald Reagent (100 mM, dissolved in NaOH 2N) was added to each well and plates were vigorously shaken for 15 min. Finally, color development was recorded at 550 nm in the plate reader. The values were normalized against the parent type of the corresponding plate. To rule out the selection of false positives, two re-screenings were carried out as described elsewhere.^[3]

Expression and purification of *S. cerevisiae* UPO variants (Fett, A77T, A77N and SoLo-A77L): UPO variants were produced and purified as described before.^[4]

Initial turnover numbers

An appropriate amount of purified enzyme was used to measure the initial turnover numbers against ABTS, NBD, veratryl alcohol, benzyl alcohol, and naphthalene. The reaction mixtures contained: 100 mM sodium citrate-phosphate pH 4.0 with 0.3 mM ABTS (molar extinction coefficient at 418 nm ϵ_{418} 36 mM⁻¹cm⁻¹) and 2 mM H₂O₂; 100 mM potassium phosphate pH 6.0/7.0 with 1 mM NBD (ϵ_{425} 9.7 mM⁻¹cm⁻¹) in 20% (v/v) acetonitrile and 1 mM H₂O₂; 100 mM potassium phosphate pH 7.0 with 100 mM veratryl alcohol (ϵ_{310} 9.3 mM⁻¹cm⁻¹) and 2 mM H₂O₂; 100 mM potassium phosphate pH 7.0 with 25 mM benzyl alcohol (ϵ_{280} 1.4 mM⁻¹cm⁻¹) and 2 mM H₂O₂; 100 mM potassium phosphate pH 7.0 with 1 mM naphthalene (ϵ_{303} 2.01 mM⁻¹cm⁻¹) in 20% (v/v) acetonitrile and 1 mM H₂O₂. The assays were carried out in 96-wells microplates, with a final volume of 200 μ L, and differences in absorbance were measured in the plate reader.

Enzymatic reactions

Saturated lauric (C₁₂), myristic (C₁₄), palmitic (C₁₆) and stearic (C₁₈) acids, unsaturated palmitoleic (C_{16:1}) and oleic (C_{18:1}) acids, fatty acid methyl esters Me-C₁₆, Me-C₁₈, Me-C_{16:1}, Me-C_{18:1} and linear alkane tetradecane were used as substrates of AaeUPO and their variants. Reactions were performed at 0.1 mM substrate concentration and 0.1-0.5 μ M enzyme in 50 mM potassium phosphate pH 7.0 at 30°C and 30-60 min reaction time, in the presence of 0.5-5 mM H₂O₂. Prior to use, the substrates were dissolved in acetone and added to the buffer to reach a final acetone concentration of 20% (v/v). In control experiments, substrates were treated under the same conditions (including 2.5-5 mM H₂O₂) without enzyme. Products were recovered by liquid-liquid extraction with methyl *tert*-butyl ether and dried under N₂. N,O-bis(trimethylsilyl)trifluoroacetamide (Supelco) was used to prepare trimethylsilyl derivatives that were analyzed by GC-MS.

GC-MS analyses

Chromatographic analyses were performed with a Shimadzu GC-MS QP2010 Ultra equipment, using a fused-silica DB-5HT capillary column (30 m x 0.25 mm internal diameter, 0.1 μ m film thickness) from J&W Scientific. The oven was heated from 120°C (1 min) to 300°C (15 min) at 5°C·min⁻¹. The injection was performed at 300°C and the transfer line was kept at 300°C. Compounds were identified by mass fragmentography as previously reported by the authors^[5, 6], and comparing their mass spectra with those of the Wiley and NIST libraries, and authentic standards. Quantifications were obtained from total-ion peak areas, using external standard curves and molar response factors of the same or similar compounds.

Overproduction of Fett_{pic} in fed-batch bioreactor and purification

Cloning and expression of Fett in *Pichia pastoris* X-33 (Fett_{pic}) was performed as described elsewhere^[7] and selection of a “high copy number” clone following a published protocol.^[8]

P. pastoris clone containing Fett was cultivated in a 30-liter bioreactor (Biostat C plus; Sartorius Stedim, Germany) adapted to the *Pichia* fermentation process guidelines of Invitrogen (version B 053002; Thermo). Basal salts medium (BMG) for the bioreactor with an initial volume of 12 L contained 26.7 mL/L 85% phosphoric acid, 0.93 g/L CaSO₄·2H₂O, 14.9 g/L MgSO₄·7H₂O, 18.2 g/L K₂SO₄, 4.13 g/L KOH, and 40 g/L glycerol. The *Pichia* trace metal salt solution (PTM1) was sterilized by filtration and consists of the following ingredients: 6 g/L CuSO₄·5H₂O, 0.08 g/L NaI, 3 g/L

MnSO₄·xH₂O, 0.2 g/L Na₂MoO₄, 0.02 g/L H₃BO₃, 0.5 g/L CoCl₂, 20 g/L ZnCl₂, 65 g/L FeSO₄·xH₂O, 0.2 g/L biotin, and 5 mL/L sulfuric acid. After autoclaving the bioreactor with the medium, 4.35 mL/L PTM1 trace salts and 1 mL antifoam B (Sigma-Aldrich, Germany) were added. The pH was adjusted to 5.0 with an ammonium hydroxide solution (NH₄OH, 28%) and was kept constant during cultivation. The fermentation process was started by adding 900 mL of a *P. pastoris* preculture grown on BMG medium including 25 µg/mL Zeocin in 500-mL baffled Erlenmeyer flasks at 180 rpm at 30°C for 24 h. The glycerol batch was run at 500 rpm at 30°C. After the completion of the glycerol phase, indicated by the peak of dissolved dioxygen (DO) after 18 to 24 h, the glycerol feed started by adding 900 mL 50% (wt/vol) glycerol containing 12 mL/L PTM1 trace salts (the DO should be kept above 20%) at 600 rpm. Subsequently, the methanol feed started by adding 3.6 mL/h/L methanol (total 8.9 L containing 12 mL/L PTM1 trace salts). Within the first 2 to 3 h, the addition of methanol was slowly increased so that the culture could adapt and the DO spike would stay above 80%. Samples were taken regularly and tested for UPO activity with ABTS as substrate and optical density (OD) at 600 nm. After 12 days of cultivation a slow decrease of enzyme activity could be detected (**Supplementary Fig. S13**) and the culture (approx. 17 L) was harvested. The supernatant containing the Fett_{pic} was separated from the cells by centrifugation at 4,600g for 20 min at 4°C. The supernatant was concentrated by ultrafiltration using tangential-flow cassettes (Sartocon slice cassette, Hydrosart, 10-kDa cut-off; Sartorius Stedim, Germany) to approx. 690 mL (798 U_{ABTS}/mL) and subsequently lyophilized for storage at -20°C (76.4 g).

Fett_{pic} mutant was purified by hydrophobic interaction chromatography (HIC) on phenyl Sepharose FF (GE Healthcare Europe GmbH, Germany) in an XK 26 x 200-mm column. 20 g of lyophilized Fett_{pic} were dissolved stepwise in eluent B (20 mM Bis-Tris pH 7.0, 226 g/L ammonium sulphate/ NH₄SO₄), loaded onto the column and bound proteins were eluted with a linear gradient from 40% to 0% ammonium sulphate. Chromatography was accomplished with an ÄKTA purifier FPLC system (GE Healthcare). Fractions with high absorption values at 420 nm (Soret band of UPOs) were measured for UPO activity with ABTS as substrate. Respective fractions were pooled and prepared for a second chromatographic step using ion exchange chromatography (IEC) on Q-Sepharose FF 26/20. IEC was carried out with Bis-Tris buffer (20 mM, pH 7.0) eluting the proteins with a linearly increasing sodium chloride gradient up to 2 M NaCl. UPO-containing fractions were pooled, dialyzed against Bis-Tris buffer and lyophilized (about 84 U_{ABTS}/mg). The homogeneity of the final Fett_{pic} mutant preparation was proven by SDS-PAGE using precast gels (Invitrogen NuPAGE Bis-Tris 10 or 12%, **Supplementary Fig. S14**).

Crystallization and structure determination of Fett_{pic} complexes

The purified Fett mutant expressed in *P. pastoris* was deglycosylated with Endo H. The released sugars and Endo H were eliminated by spinning with a 30 kDa filtration membrane and protein was concentrated to 10.5 mg/ml in 50 mM sodium citrate pH 5.6 buffer. Crystals were obtained by reproducing previous conditions applied to AaeUPO mutant PaDa-I^[9] and they were grown by the hanging-drop vapour-diffusion method at 18°C. After three weeks, several crystals were obtained in 1.35-1.6M sodium phosphate buffer (pH 5.6) with 3-5% 2-methyl-2,4-pentanediol (MPD) and protein:reservoir ratio of 2:1.

Diffraction data were collected in XALOC beamline at ALBA synchrotron (Barcelona, Spain). Data were integrated and scaled with XDS^[10] and then merged with AIMLESS program from the CCP4 package.^[11] These crystals belong to P2₁ space group containing one molecule per asymmetric unit (mol/ASU) and 47 % of solvent content within the unit cell. The structure of the Fett mutant was solved by difference Fourier synthesis using the coordinates of the evolved UPO crystals.^[9] For automated refinement, REFMAC^[10] within the CCP4 suite was used, followed by model building using Coot.^[11] Rigid body refinement was carried out at the first steps and then, restrain refinement was held. Free R-factor was calculated using a subset of 5% randomly selected structure-factor amplitudes that were excluded from automated refinement. At the later steps, N-acetylglucosamine and water molecules were added, which, combined with more rounds of restrained refinement, led to the final statistics reported in **Table S3**.

Eight peroxidase and peroxygenase substrates were used, all of them being dissolved in methanol. Pre-formed Fett crystals were soaked in the precipitant solution, supplemented with 10 to 50 mM ligand for one to 36 hours. The crystals were then cryoprotected with 25 % v/v glycerol prior to diffraction experiments carried out in XALOC at the Alba synchrotron. The complexes were solved by Fourier transformations using the coordinates from the unsubstituted form and substrate ligands, solvent molecules and waters were manually fitted into the density with Coot. For MLA, not described in the Protein Data Bank (PDB), restrain files were generated with CSD Mogul in PHENIX program.^[12] Soaking with ABTS was unsuccessful showing no density at the active site. Details for the complexes with hexane, tetradecane, naphthalene, lauric acid, 12-methoxylauric (MLA), myristic acid and palmitoleic acid are provided in **Table S3**. Verification of these structures was done via PDB Validation server (validate.wwpdb.org) before coordinates and associated structure factors were deposited in PDB. The structural figures were prepared with PyMOL.

Accession codes: Atomic coordinates and structure factors of the Fett complexes have been deposited in the Protein Data Bank (PDB), with the following codes: 7PN4 (Naphthalene), 7PN5 (Hexane), 7PN6 (Myristic acid), 7PN7 (Palmitoleic acid), 7PN8 (Tetradecane), 7PN9 (Lauric acid) and 7PNA (12-methoxylauric acid).

Computational methods

System setup. A high-resolution crystal structure of Fett with myristic acid (MA) as a substrate was used to prepare two models of the AaeUPO and Fett variants. For the purpose of this work, the heme cofactor present in the structure was modified to a reactive oxo ferryl cation radical complex (+•Heme-Fe⁴⁺=O), Compound I (CPDI). AMBER force field^[13] parameters for CPDI and Cys36 involved in the Fe-coordination sphere were prepared based on data provided by Cheatham and co-workers.^[14] Magnesium ion (Mg²⁺) parameters were taken from the study of Villa and co-workers.^[15] Subsequently, missing AMBER FF parameters for N-acetylglucosamine (NAG) bound to asparagine residues (Asn11, Asn141, Asn161, Asn182, and Asn286 of the polypeptide chain), as well as parameters for both substrates (*i.e.*, myristic acid (MA) and ω-1-hydroxymyristic acid (ω-1-OH-MA)) were generated employing Generalized Amber Force Field (GAFF)^[16] using the Antechamber software.^[17] All newly produced parameters are provided in **Tables S4-S7**. The pKa shift of all titratable residues was determined with PropKa software ver. 3.1.^[18, 19] Importantly, the

computed pKa values are neither affected by the mutation of Ala77 to Leu nor by type of the substrates used in this work. As shown in **Fig. S17** apart from Asp85 and His118, with pKa of 7.27 and 8.60, respectively, all remaining residues were found in their natural protonated state at neutral pH 7.0. After geometrical inspection histidine residues such as His22, His45, His82, and His138 were protonated in δ -, while His-251 was in ϵ -position. In addition, the existence of one disulfide bridge formed between Cys278 and Cys319 was detected, therefore no hydrogens were assigned to bind to S^Y atoms of these residues.

Then, missing hydrogen atoms were added to the enzyme, cofactor, and substrate together with 3 positively charged sodium (Na⁺) counterions that were put in the most electrostatically favorable positions to neutralize the total negative charge of the system. Hydrogen and counterions were added using the tLEAP^[18] module of the AmberTools package. Subsequently, the system was soaked within an orthorhombic box of TIP3P^[19] water molecules, with an average size of 84 × 88 × 77 Å³. To describe the protein and water molecules the AMBER ff03.r1 and TIP3P force fields, respectively, were employed and the NAMD^[20] software was used as a molecular dynamic (MD) engine. A cut-off for non-bonding interactions was set between 14.5 to 16 Å using a smooth switching function. The temperature during the simulations was controlled using the Langevin thermostat,^[21] and the pressure with the Nosé-Hoover Langevin piston^[22] pressure control. In all simulations, periodic boundary conditions (PBC) were applied.

MD simulations. The equilibration protocol for MD simulations involved a preliminary minimization and gradual heating of the system to 303.15 K with 0.001 K temperature increments, followed by 100 ps of non-biased NPT equilibration. In the case of AaeUPO and Fett variants with MA substrate, MD simulations were divided into two phases. In the first phase, the distance between the Fe=O group and C13 of the substrate was constrained during 10 ns of MD simulations (distance $d(\text{Fe}=\text{O}\cdots\text{C13}) = 2.5$ Å with force constant, $k_{(\text{Fe}=\text{O}\cdots\text{C13})} = 500.0$ kcal·mol⁻¹·Å⁻²). This approach was employed because of the original distal position of the substrate in the binding channel observed in the crystal structure. The last generated structure in this step was then used in the second phase, where 0.5 μs of no-restricted MD simulations were done. Due to the possible bias of starting point generated by substrate position enforcement, the first 100 ns of no-restricted NPT MD simulations were dedicated to system equilibration, and therefore the results from the last 400 ns of simulations were taken into account during results analysis. The initial structure used as a starting point in the second phase was additionally prepared as a starting point for MD simulations of AaeUPO and Fett variants with alternative ω-1-OH-MA substrate. As this simulation may be accompanied by diffusion of the new substrate from the binding channel, we decided to run a longer MD simulation, *i.e.*, 1 μs to confirm or exclude the possibility of ω-1-OH-MA unbinding. In this case, analysis was based on results generated along the complete MD simulations.

Semi-preparative scale transformation of myristic acid using Fett_{pic}

Two different approaches were tested using acetone (cosolvent 1) or *tert*-butanol (cosolvent 2) as cosolvents.

Cosolvent 1. Myristic acid was dissolved in buffer phosphate (50 mM, pH 7.0) containing 60% acetone giving a concentration of 50 mM. The solution was heated at 30 °C, Fett_{pic} (25 μM) was added and the reaction was triggered using H₂O₂ as oxidant

(0.5 M) supplied with a syringe pump during 50 min of total reaction time of 1h. Products were extracted with methyl *tert*-butyl ether and subjected to GC-MS analysis. Total reaction volumes of 0.5-2.0 were satisfactory assayed.

Cosolvent 2. 12 g (SCU-1) or 6 g (SCU-2) of ground myristic acid were suspended in 123 ml t-BuOH and 410 ml KPi buffer (100 mM pH 7.0) and supplemented with Fett_{pic} (0.2 μM initial concentration and supplemented at intervals to reach the final concentration of 1.2 μM (SCU-1) or 4 μM (SCU-2)). The reactions were initiated by starting a continuous feed of H₂O₂ (1 mM/h from a 100 mM stock solution using a syringe pump). The reactions were terminated after 164h by acidification of the reaction mixture to approx. pH 3.1. The crude product mixture were filtrated, washed with warm MTBE (50 mL, to remove salt impurities) and purified via flash chromatography using petrol ether (40/60):MTBE (3:1) as eluent. The isolated yields were 1.38 g (SCU-1) and 1.2 g (SCU-2) of essentially pure 13-hydroxy myristic acid, respectively. The crude and purified products were analyzed using ¹H-NMR in agreement with reported literature.^[23]

References

- [1] A. Faig, L. K. Petersen, P. V. Moghe, K. E. Uhrich, *Biomacromolecules* **2014**, *15*, 3328–3337.
- [2] M. Alcalde, in *In Vitro Mutagenesis Protocols* (Ed.: J. Braman), Humana Press, Totowa, NJ, **2010**, pp. 3–14.
- [3] P. Molina-Espeja, E. Garcia-Ruiz, D. Gonzalez-Perez, R. Ullrich, M. Hofrichter, M. Alcalde, *Appl Environ Microbiol* **2014**, *80*, 3496–3507.
- [4] P. Gomez de Santos, M. Cañellas, F. Tieves, S. H. H. Younes, P. Molina-Espeja, M. Hofrichter, F. Hollmann, V. Guallar, M. Alcalde, *ACS Catal.* **2018**, *8*, 4789–4799.
- [5] A. Gutiérrez, E. D. Babot, R. Ullrich, M. Hofrichter, A. T. Martínez, J. C. del Río, *Archives of Biochemistry and Biophysics* **2011**, *514*, 33–43.
- [6] E. D. Babot, J. C. del Río, L. Kalum, A. T. Martínez, A. Gutiérrez, *Biotechnol. Bioeng.* **2013**, *110*, 2323–2332.
- [7] P. Molina-Espeja, M. Cañellas, F. J. Plou, M. Hofrichter, F. Lucas, V. Guallar, M. Alcalde, *ChemBioChem* **2016**, *17*, 341–349.
- [8] P. Gomez de Santos, M. D. Hoang, J. Kiebist, H. Kellner, R. Ullrich, K. Scheibner, M. Hofrichter, C. Liers, M. Alcalde, *Appl Environ Microbiol* **2021**, *87*, e00878-21.
- [9] M. Ramirez-Escudero, P. Molina-Espeja, P. Gomez de Santos, M. Hofrichter, J. Sanz-Aparicio, M. Alcalde, *ACS Chem. Biol.* **2018**, *13*, 3259–3268.
- [10] W. Kabsch, *Acta Crystallographica Section D: Biological Crystallography* **2010**, *66*, 125–132.
- [11] P. R. Evans, G. N. Murshudov, *Acta Crystallogr D Biol Crystallogr* **2013**, *69*, 1204–1214.
- [12] P. D. Adams, P. V. Afonine, G. Bunkóczi, V. B. Chen, N. Echols, J. J. Headd, L.-W. Hung, S. Jain, G. J. Kapral, R. W. Grosse-Kunstleve, A. J. McCoy, N. W. Moriarty, R. D. Oeffner, R. J. Read, D. C. Richardson, J. S. Richardson, T. C. Terwilliger, P. H. Zwart, *Methods* **2011**, *55*, 94–106.
- [13] Duan, Y.; Wu, C.; Chowdhury, S.; Lee, M.C.; Xiong, G.; Zhang, W.; Yang, R.; Cieplak, P.; Luo, R.; Lee, T.; et al. *J. Comput. Chem.* **2003**, *24*, 1999–2012.
- [14] K. Shahrokh, A. Orendt, G. S. Yost, T. E. Cheatham, III, *J. Comput. Chem.* **2012**, *33*, 119-133.
- [15] O. Allnér, L. Nilsson, A. Villa *J. Chem. Theory Comput.* **2012**, *8*, 1493-1502.
- [16] Wang, J., Wolf, R. M.; Caldwell, J. W.; Kollman, P. A.; Case, D. A. *J. Comput. Chem.* **2004**, *25*, 1157-1174.
- [17] Wang, J.; Wang, W.; Kollman, P.A.; Case, D.A. **2006**, *25*, 247–260.
- [18] Søndergaard, C.R.; Olsson, M.H.M.; Rostkowski, M.; Jensen, J.H. *J. Chem. Theory Comput.* **2011**, *7*, 2284–2295.
- [19] Olsson, M.H.M.; Søndergaard, C.R.; Rostkowski, M.; Jensen, J.H. *J. Chem. Theory Comput.* **2011**, *7*, 525–537.
- [20] Schafmeister, C.E.A.; Ross, W.S.; Romanovski, V. LEAP, University of California, San Francisco, **1995**.
- [21] Jorgensen, W.L.; Chandrasekhar, J.; Madura, J.D.; Impey, R.W.; Klein, M.L. *J. Chem. Phys.* **1983**, *79*, 926–935.
- [22] Phillips, J.C.; Braun, R.; Wang, W.; Gumbart, J.; Tajkhorshid, E.; Villa, E.; Chipot, C.; Skeel, R.D.; Kalé, L.; Schulten, K. *J. Comput. Chem.* **2005**, *26*, 1781–1802.
- [23] Tian, Y.; Liu, Z.Q. *Green Chem.* **2017**, *19*: 5230-5235.

Table S1. ^1H and ^{13}C chemical shifts for MLA.

Position number	δ_{H} (Multiplicity, J, nH)	δ_{C}
12	3.37 (t, 6.7 Hz, 2H)	73.0
14	3.34 (s, 3H)	58.5
2	2.34 (t, 7.5 Hz, 2H)	34.0
3	1.64	24.7
11	1.56 (dt, 8.0, 6.5 Hz, 2H)	29.5
10	1.28	26.1
9	1.28	29.4
8	1.28	29.6
7	1.28	29.0
6	1.28	29.4
5	1.28	29.4
4	1.28	29.2
1	-	179.5

Table S2. Relative percentage of products in the reactions of different UPO variants with fatty acids (Myristic acid, C14; Lauric acid, C12; Palmitic acid, C16; Stearic acid, C18; Palmitoleic acid, C16:1; Oleic acid, C18:1), 12-methoxylauric acid (MLA).

Substrate	Products	UPO variants				
		AaeUPO	Fett (A77L)	A77T	A77N	SoloA77L
MLA	Ald	79.0 ^g	nd ^c	13.2 ^a	nd ^{a-e}	nd ^{a-e}
	ωOH	11.0 ^g	>99.0% ^c	86.2 ^a	tr ^{a-e}	tr ^{a-e}
	Acid	10.0 ^g	nd ^c	0.6 ^a	nd ^{a-e}	nd ^{a-e}
C ₁₂	ω OH	nd ^b	2.1 ^b	6.5 ^a	nd ^{a,f}	nd ^{a,f}
	ω-1 OH	55.9 ^b	92.3 ^b	76.5 ^a	tr ^{a,f}	tr ^{a,f}
	ω-2 OH	41.7 ^b	5.6 ^b	10.5 ^a	nd ^{a,f}	nd ^{a,f}
	ω-1 keto	2.4 ^b	nd ^b	6.5 ^a	nd ^{a,f}	nd ^{a,f}
C ₁₄	ω OH	nd ^b	1.1 ^b	2.7 ^{a,b}	3.5 ^e	2.2 ^e
	ω-1 OH	45.4 ^b	95.1 ^b	82.6 ^{a,b}	93.1 ^e	93.8 ^e
	ω-2 OH	40.7 ^b	3.8 ^b	11.7 ^{a,b}	3.4 ^e	4.0 ^e
	ω-1 keto	13.9 ^b	nd ^b	3.0 ^{a,b}	nd ^{a-e}	nd ^{a-e}
C ₁₆	ω-1 OH	20.3 ^b	98.0 ^b			
	ω-2 OH	27.0 ^b	2.0 ^b			
	ω-1 keto	37.6 ^b				
	ω-2 keto	10.3 ^b				
	ω-1/ω-2 keto	4.8 ^b				
C ₁₈	ω OH	5.8 ^f	96.2 ^f			
	ω-1 OH	19.4 ^f	3.8 ^f			
	ω-2 OH	41.1 ^f				
	ω-1 keto	12.4 ^f				
	ω-2 keto	10.6 ^f				
	Acid	10.7 ^f				
C _{16:1}	ω OH	nd ^a	nd ^a	-	-	-
	ω-1 OH	35.3 ^a	88.0 ^a	-	-	-
	ω-2 OH	48.6 ^a	7.0 ^a	-	-	-
	ω-1 keto	8.1 ^a	5.0 ^a	-	-	-
	ω-2 keto	8.0 ^a	nd ^a	-	-	-
C _{18:1}	ω OH		3.1 ^b			
	ω-1 OH	12.5 ^b	90.3 ^b			
	ω-2 OH	22.0 ^b	2.7 ^b			
	ω-1 keto	56.7 ^b				
	ω-2 keto	8.8 ^b	3.9			

^a0.1 μM enzyme, 2.5 mM H₂O₂, 60 min; ^b0.1 μM enzyme, 2.5 mM H₂O₂, 30 min; ^c0.2 μM enzyme, 2.5 mM H₂O₂, 30 min; ^d0.2 μM enzyme, 5 mM H₂O₂, 30 min; ^e0.5 μM enzyme, 5 mM H₂O₂, 60 min; ^f0.5 μM enzyme, 2.5 mM H₂O₂, 60 min; ^g0.025 μM enzyme, 5 mM H₂O₂, 60 min; ^h40% acetone. nd (not detected) and tr (traces).

Table S2 (Cont.). Relative percentage of products in the reactions of different UPO variants with fatty acid methyl esters (Methyl palmitate, Me-C₁₆; Methyl stearate, Me-C₁₈; Methyl palmitoleate, Me-C_{16:1}; Methyl oleate, Me-C_{18:1}) and tetradecane.

Substrate	Products	UPO variants				
		AaeUPO	Fett (A77L)	A77T	A77N	SoloA77L
Me-C ₁₆	ω-1 OH	58.2 ^f	97.9 ^f			
	ω-2 OH	29.4 ^f	2.1 ^f			
	ω-1 keto	12.4 ^f				
Me-C ₁₈	ω-1 OH	36.6 ^f	n.d ^f			
	ω-2 OH	63.4 ^f	n.d ^f			
Me-C _{16:1}	ω-1 OH	38.2 ^f	99.0 ^f			
	ω-2 OH	61.8 ^f	1.0 ^f			
Me-C _{18:1}	ω-1 OH	61.5 ^f	100 ^f			
	ω-2 OH	38.5 ^f				
Tetradecane ^h	ω-1 OH	1.5 ^a	19.6 ^a	26.1 ^a	tr ^{a-e}	tr ^{a-e}
	ω-2 OH	4.7 ^a	1.1 ^a	12.1 ^a	nd ^{a-e}	nd ^{a-e}
	2, ω-1 diOH	18.7 ^a	70.3 ^a	39.0 ^a	nd ^{a-e}	nd ^{a-e}
	2, ω-2 diOH	36.2 ^a	9.0 ^a	19.8 ^a	nd ^{a-e}	nd ^{a-e}
	3, ω-2 diOH	19.6 ^a	nd ^a	3.0 ^a	nd ^{a-e}	nd ^{a-e}
	keto, OH	19.3 ^a	nd ^a			

^a0.1 μM enzyme, 2.5 mM H₂O₂, 60 min; ^b0.1 μM enzyme, 2.5 mM H₂O₂, 30 min; ^c0.2 μM enzyme, 2.5 mM H₂O₂, 30 min; ^d0.2 μM enzyme, 5 mM H₂O₂, 30 min; ^e0.5 μM enzyme, 5 mM H₂O₂, 60 min; ^f0.5 μM enzyme, 2.5 mM H₂O₂, 60 min; ^g0.025 μM enzyme, 5 mM H₂O₂, 60 min; ^h40% acetone. nd (not detected) and tr (traces).

Table S3. Crystallographic statistics of Fett_{pic} mutant complexes.

Crystal data	Hexane	Tetradecane	Napthalene	Lauric acid	MLA	Myristic acid	Palmitoleic acid
Space group	P2 ₁	P2 ₁	P2 ₁	P2 ₁	P2 ₁	P2 ₁	P2 ₁
Molecules/a.u.	1	1	1	1	1	1	1
Unit cell parameters							
a (Å)	51.11	51.17	50.96	51.09	51.47	51.21	51.25
b (Å)	57.96	58.00	57.65	57.78	58.08	57.91	57.00
c (Å)	60.80	60.86	60.63	60.86	61.20	61.12	60.97
β (°)	109.17	110.08	109.44	109.50	109.93	109.46	109.83
Data collection							
Beamline	XALOC (ALBA)	XALOC (ALBA)	XALOC (ALBA)	XALOC (ALBA)	XALOC (ALBA)	XALOC (ALBA)	XALOC (ALBA)
Temperature (K)	100	100	100	100	100	100	100
Wavelength (Å)	0.9793	0.9793	0.9793	0.9793	0.9793	0.9793	0.9793
Resolution (Å)	44.93-1.82 (1.86-1.82)	48.06-1.50 (1.53-1.50)	48.05-2.05 (2.11-2.05)	48.16-1.85 (1.89-1.85)	48.38-1.90 (1.94-1.90)	48.28-1.50 (1.53-1.50)	48.21-1.65 (1.68-1.65)
Data processing							
Total reflections	186576 (11389)	346868 (15965)	140057 (10881)	154967 (8852)	177714 (11386)	357827 (17743)	257566 (11322)
Unique reflections	30212 (1767)	53317 (2617)	20970 (1622)	27775 (1611)	26835 (1687)	54034 (2700)	40293 (1903)
Multiplicity	6.2 (6.4)	6.5 (6.1)	6.7 (6.7)	5.6 (5.5)	6.6 (6.7)	6.6 (6.6)	6.4 (5.9)
Completeness (%)	99.9 (99.9)	99.8 (98.5)	100 (100)	97.6 (91.2)	99.8 (99.4)	99.9 (100)	99.7 (95.7)
Mean I/σ (I)	6.7 (2.8)	13.6 (4.3)	9.7 (3.8)	13.4 (3.1)	10.1 (4.4)	15.1 (5.6)	10.2 (4.1)
R _{merge} [†] (%)	26.7 (70.7)	11.3 (46.5)	17.0 (66.8)	12.4 (57.5)	18.2 (68.0)	10.6 (64.2)	16.6 (51.1)
R _{pim} ^{††} (%)	12.0 (30.7)	4.8 (20.2)	7.1 (28.1)	6.1 (26.6)	7.7 (28.1)	4.4 (27.4)	7.2 (22.7)
Refinement							
R _{work} / R _{free} ^{†††} (%)	22.0/26.9	15.0/16.4	16.8/20.9	24.7/27.7	16.4/19.6	16.3/18.9	16.3/18.7
N° of atoms/aver. B (Å²)							
Protein	2574/20.77	2574/12.84	2574/25.55	2566/16.54	2551/18.09	2574/12.87	2574/16.73
Ligands	118/26.17	140/21.45	126/36.81	126/25.93	136/24.46	136/24.11	138/25.12
Solvent	253/30.18	244/22.52	169/30.28	234/26.63	133/24.18	222/21.36	198/24.71
All atoms	2945/21.79	2958/14.05	2869/26.32	2926/17.75	2820/18.69	2932/14.04	2910/17.67
Ramachandran plot (%)							
Favoured	93.4	94.1	94.7	94.1	93.6	94.1	94.4
Outliers	0.66	0.99	0.99	1.34	0.96	0.99	0.99
RMS deviations							
Bonds (Å)	0.006	0.008	0.006	0.007	0.01	0.009	0.007
Angles (°)	1.372	1.480	1.373	1.462	1.473	1.492	1.471
PDB accession codes							
	7PN5	7PN8	7PN4	7PN9	7PNA	7PN6	7PN7

Values in brackets are for the high-resolution shell

[†]R_{merge} = $\sum hkl \sum_i |I_i(hkl) - [I(hkl)]| / \sum hkl \sum_i I_i(hkl)$, where $I_i(hkl)$ is the i th measurement of reflection hkl and $[I(hkl)]$ is the weighted mean of all measurements.

^{††}R_{pim} = $\sum hkl [1/(N - 1)]^{1/2} \sum_i |I_i(hkl) - [I(hkl)]| / \sum hkl \sum_i I_i(hkl)$, where N is the redundancy for the hkl reflection.

^{†††}R_{work} / R_{free} = $\sum hkl |F_o - F_c| / \sum hkl |F_o|$, where F_c is the calculated and F_o is the observed structure factor amplitude of reflection hkl for the working / free (5%) set, respectively.

Table S4. Force field parameters for the Asn-NAG covalent adduct generated based on GAFF as available in Antechamber software together with the partial charges computed at AM1 level of theory.

NON-BOND			r	Epsilon
NT			1.8240	0.1700
H			0.6000	0.0157
CT			1.9080	0.1094
C			1.9080	0.0860
N			1.8240	0.1700
OS			1.6837	0.1700
OH			1.7210	0.2104
HO			0.0000	0.0000
H1			1.3870	0.0157
HC			1.4870	0.0157
O			1.6612	0.2100
H2			1.2870	0.0157

Atom name	Atom Type	Charge	Atom name	Atom Type	Charge
N	N	-0.872503	O3	OH	-0.557094
HT1	H	0.372005	H9	HO	0.419190
CA	CT	0.063498	H3	H1	0.103971
CB	CT	-0.185182	N2	N	-0.540743
CG	C	0.691869	C7	C	0.688772
ND2	N	-0.538808	C8	CT	-0.168444
C1	CT	0.302002	H81	HC	0.072653
C2	CT	0.044087	H82	HC	0.072653
C3	CT	0.137424	H83	HC	0.072653
C4	CT	0.087865	O7	O	-0.610598
C5	CT	0.072377	H10	H	0.335042
O5	OS	-0.433059	H2	H1	0.085387
C6	CT	0.142896	H1	H2	0.092614
O6	OH	-0.570639	HD2	H	0.352594
H6	HO	0.433644	OD1	O	-0.594150
H61	H1	0.053380	HB1	HC	0.079708
H62	H1	0.053380	HB2	HC	0.079708
H5	H1	0.079192	HA	H1	0.095712
O4	OH	-0.559029	C	C	0.588414
H7	HO	0.421255	O	O	-0.511911
H4	H1	0.048217			

MASS		ANGLE	
N	14.010 0.530	CT-CT-N	80.000 111.200
H	1.008 0.161	H1-CT-N	50.000 109.500
CT	12.010 0.878	C-CT-N	80.000 111.200
C	12.010 0.616	CT-N-H	50.000 109.500
N	14.010 0.530	C-CT-CT	63.000 111.100
OS	16.000 0.465	CT-CT-HC	50.000 109.500
OH	16.000 0.465	CT-C-O	80.000 120.400
HO	1.008 0.135	CT-CT-H1	50.000 109.500
H1	1.008 0.135	CT-C-N	70.000 116.600
HC	1.008 0.135	C-CT-HC	50.000 109.500
O	16.000 0.434	C-N-CT	50.000 121.900
H2	1.008 0.135	C-N-H	50.000 120.000
		N-C-O	80.000 122.900
		CT-CT-N	80.000 109.700
		N-CT-OS	0.000 0.000
		H2-CT-N	50.000 109.500
		CT-N-H	50.000 118.040
		CT-CT-CT	40.000 109.500
		CT-OS-CT	60.000 109.500
		CT-CT-OS	50.000 109.500
		CT-CT-H2	50.000 109.500
		CT-CT-OH	50.000 109.500
		CT-OH-HO	55.000 108.500
		H2-CT-OS	50.000 109.500

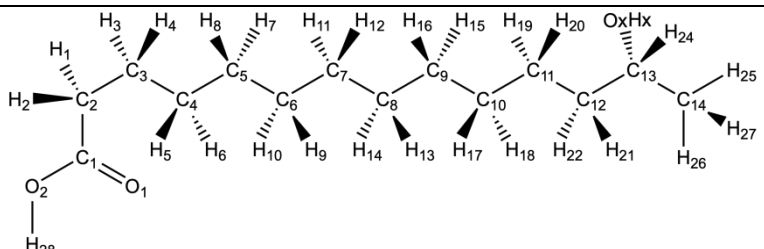
BOND	
H-N	434.00 1.010
CT-N	367.00 1.471
CT-CT	310.00 1.526
CT-H1	340.00 1.090
C-CT	317.00 1.522
CT-HC	340.00 1.090
C-N	490.00 1.335
C-O	570.00 1.229
CT-N	337.00 1.449
H-N	434.00 1.010
CT-OS	320.00 1.410

CT-H2 340.00 1.090	H1-CT-OS 50.000 109.500
CT-OH 320.00 1.410	H1-CT-OH 50.000 109.500
HO-OH 553.00 0.960	H1-CT-H1 35.000 109.500
	H1-CT-N 50.000 109.500
	HC-CT-HC 35.000 109.500
	C-CT-H1 50.000 109.500
DIHEDRALS	DIHEDRALS
C-CT-CT-N 9 1.400 0.000 3.000	H1-CT-OH-HO 3 0.500 0.000 3.000
HC-CT-CT-N 9 1.400 0.000 3.000	H1-CT-OS-CT 3 1.150 0.000 3.000
O-C-CT-N 6 0.000 0.000 2.000	H1-CT-CT-OH 1 0.000 0.000 -3.000
CT-CT-N-H 6 1.800 0.000 3.000	H1-CT-CT-OH 1 0.250 0.000 1.000
H1-CT-N-H 6 1.800 0.000 3.000	H1-CT-CT-H1 9 1.400 0.000 3.000
C-CT-N-H 6 1.800 0.000 3.000	OH-CT-CT-OH 1 0.144 0.000 -3.000
N-C-CT-CT 1 0.000 0.000 -4.000	OH-CT-CT-OH 1 1.175 0.000 2.000
N-C-CT-CT 1 0.400 0.000 -3.000	N-CT-CT-OH 1 0.000 0.000 -1.000
N-C-CT-CT 1 0.200 0.000 -2.000	N-CT-CT-OH 1 1.490 0.000 -2.000
N-C-CT-CT 1 0.200 0.000 1.000	N-CT-CT-OH 1 0.156 0.000 -3.000
O-C-CT-CT 6 0.000 0.000 2.000	N-CT-CT-OH 1 0.000 0.000 4.000
CT-C-N-CT 4 10.000 180.000 2.000	N-C-CT-HC 6 0.000 0.000 2.000
CT-C-N-H 4 10.000 180.000 2.000	O-C-CT-HC 1 0.800 0.000 -1.000
CT-CT-N-C 1 0.000 0.000 -4.000	O-C-CT-HC 1 0.000 0.000 -2.000
CT-CT-N-C 1 0.400 0.000 -3.000	O-C-CT-HC 1 0.080 180.000 3.000
CT-CT-N-C 1 2.000 0.000 -2.000	O-C-N-H 1 2.500 180.000 -2.000
CT-CT-N-C 1 2.000 0.000 1.000	O-C-N-H 1 2.000 0.000 1.000
OS-CT-N-C 6 0.000 0.000 2.000	H1-CT-N-C 6 0.000 0.000 2.000
H2-CT-N-C 6 0.000 0.000 2.000	H1-CT-N-H 6 0.000 0.000 2.000
CT-CT-CT-N 9 1.400 0.000 3.000	CT-CT-CT-H2 9 1.400 0.000 3.000
N-CT-CT-N 9 1.400 0.000 3.000	H2-CT-CT-N 9 1.400 0.000 3.000
H1-CT-CT-N 9 1.400 0.000 3.000	H1-CT-CT-H2 9 1.400 0.000 3.000
N-CT-OS-CT 3 1.150 0.000 3.000	H2-CT-OS-CT 3 1.150 0.000 3.000
CT-CT-CT-CT 1 0.180 0.000 -3.000	OS-CT-N-H 6 0.000 0.000 2.000
CT-CT-CT-CT 1 0.250 180.000 -2.000	H2-CT-N-H 6 0.000 0.000 2.000
CT-CT-CT-CT 1 0.200 180.000 1.000	C-CT-CT-H1 9 1.400 0.000 3.000
CT-CT-CT-OH 9 1.400 0.000 3.000	H1-CT-CT-HC 9 1.400 0.000 3.000
CT-CT-CT-H1 9 1.400 0.000 3.000	O-C-CT-H1 1 0.800 0.000 -1.000
CT-CT-N-H 6 0.000 0.000 2.000	O-C-CT-H1 1 0.000 0.000 -2.000
CT-CT-OS-CT 1 0.383 0.000 -3.000	O-C-CT-H1 1 0.080 180.000 3.000
CT-CT-OS-CT 1 0.100 180.000 2.000	C-CT-CT-C 9 1.400 0.000 3.000
CT-CT-OH-HO 1 0.160 0.000 -3.000	C-CT-CT-HC 9 1.400 0.000 3.000
CT-CT-OH-HO 1 0.250 0.000 1.000	
O-C-N-CT 4 10.000 180.000 2.000	IMPROPERS
CT-CT-CT-OS 9 1.400 0.000 3.000	CT-N-C-O 10.5 180.0 2.0
N-CT-CT-OS 9 1.400 0.000 3.000	C-CT-N-H 1.1 180.0 2.0
H1-CT-CT-OS 1 0.000 0.000 -3.000	
H1-CT-CT-OS 1 0.250 0.000 1.000	
OH-CT-CT-OS 1 0.144 0.000 -3.000	
OH-CT-CT-OS 1 1.175 0.000 2.000	

Table S5. Force field parameters for the myristic acid (MA) substrate generated based on GAFF as available in Antechamber software together with the partial charges computed at AM1 level of theory.

Atom name	Atom Type	Charge	Atom name	Atom Type	Charge				
O1	o	-0.551000	C8	c3	-0.077400				
C1	c	0.634100	H13	hc	0.038700				
O2	oh	-0.612100	H14	hc	0.038700				
H28	ho	0.443000	C9	c3	-0.076400				
C2	c3	-0.126400	H15	hc	0.038700				
H1	hc	0.080200	H16	hc	0.038700				
H2	hc	0.080200	C10	c3	-0.076400				
C3	c3	-0.079400	H17	hc	0.038700				
H3	hc	0.057700	H18	hc	0.038700				
H4	hc	0.057700	C11	c3	-0.077400				
C4	c3	-0.079400	H19	hc	0.038700				
H5	hc	0.045200	H20	hc	0.038700				
H6	hc	0.045200	C12	c3	-0.082400				
C5	c3	-0.080400	H21	hc	0.041200				
H7	hc	0.039700	H22	hc	0.041200				
H8	hc	0.039700	C13	c3	-0.080400				
C6	c3	-0.078400	H23	hc	0.038200				
H9	hc	0.040200	H24	hc	0.038200				
H10	hc	0.040200	C14	c3	-0.092100				
C7	c3	-0.082400	H25	hc	0.032367				
H11	hc	0.042700	H26	hc	0.032367				
H12	hc	0.042700	H27	hc	0.032367				
NON-BOND			MASS						
o	1.6612	0.2100	o	16.000	0.434				
c	1.9080	0.0860	c	12.010	0.616				
oh	1.7210	0.2104	oh	16.000	0.465				
ho	0.0000	0.0000	ho	1.008	0.135				
c3	1.9080	0.1094	c3	12.010	0.878				
hc	1.4870	0.0157	hc	1.008	0.135				
BOND			ANGLE						
c-o	637.70	1.218	o-c-oh	75.900	122.100				
c-oh	400.10	1.351	c3-c-o	67.400	123.200				
c-c3	313.00	1.524	c-oh-ho	49.900	106.550				
ho-oh	371.40	0.973	c-c3-hc	46.900	108.770				
c3-hc	330.60	1.097	c-c3-c3	63.300	111.040				
c3-c3	300.90	1.538	c3-c-oh	68.400	112.730				
			c3-c3-hc	46.300	109.800				
			c3-c3-c3	62.900	111.510				
			hc-c3-hc	39.400	107.580				
DIHEDRAL			DIHEDRAL						
o-c-oh-ho	1	2.300	180.000	-2.000	c3-c3-c3-c3	1	0.180	0.000	-3.000
o-c-oh-ho	1	1.900	0.000	1.000	c3-c3-c3-c3	1	0.250	180.000	-2.000
o-c-c3-hc	1	0.800	0.000	-1.000	c3-c3-c3-c3	1	0.200	180.000	1.000
o-c-c3-hc	1	0.000	0.000	-2.000	hc-c3-c3-hc	1	0.150	0.000	3.000
o-c-c3-hc	1	0.080	180.000	3.000	c-c3-c3-hc	9	1.400	0.000	3.000
o-c-c3-c3	6	0.000	180.000	2.000	c-c3-c3-c3	9	1.400	0.000	3.000
IMPROPER			IMPROPER						
c3-o-c-oh	1.1	180.0	2.0	oh-c-c3-hc	6	0.000	180.000	2.000	
				oh-c-c3-c3	6	0.000	180.000	2.000	
				c3-c-oh-ho	2	4.600	180.000	2.000	
				c3-c3-c3-hc	1	0.160	0.000	3.000	

Table S6. Force field parameters for the ω -1-OH myristic acid (ω -1-OH-MA) substrate generated based on GAFF as available in Antechamber software together with the partial charges computed at AM1 level of theory.



Atom name	Atom Type	Charge	Atom name	Atom Type	Charge				
O1	o	-0.551000	H14	hc	0.039700				
C1	c	0.635100	H13	hc	0.039700				
O2	oh	-0.612100	C9	c3	-0.078400				
H28	ho	0.444000	H16	hc	0.039700				
C2	c3	-0.126400	H15	hc	0.039700				
H2	hc	0.079700	C10	c3	-0.079400				
H1	hc	0.079700	H18	hc	0.041200				
C3	c3	-0.080400	H17	hc	0.041200				
H4	hc	0.058200	C11	c3	-0.077400				
H3	hc	0.058200	H20	hc	0.041200				
C4	c3	-0.078400	H19	hc	0.041200				
H5	hc	0.041200	C12	c3	-0.113400				
H6	hc	0.041200	H22	hc	0.046700				
C5	c3	-0.079400	H21	hc	0.046700				
H8	hc	0.042700	C13	c3	0.141100				
H7	hc	0.042700	OX	oh	-0.601800				
C6	c3	-0.079400	HX	ho	0.397000				
H10	hc	0.039700	H24	h1	0.029700				
H9	hc	0.039700	C14	c3	-0.090100				
C7	c3	-0.079400	H26	hc	0.045033				
H11	hc	0.040700	H25	hc	0.045033				
H12	hc	0.040700	H27	hc	0.045033				
C8	c3	-0.078400							
NON-BOND			MASS						
o	1.6612	0.2100	o	16.000	0.434				
c	1.9080	0.0860	c	12.010	0.616				
oh	1.7210	0.2104	oh	16.000	0.465				
ho	0.0000	0.0000	ho	1.008	0.135				
c3	1.9080	0.1094	c3	12.010	0.878				
hc	1.4870	0.0157	hc	1.008	0.135				
h1	1.3870	0.0157	h1	1.008	0.135				
BOND			ANGLE						
c-o	637.70	1.218	o-c-oh	75.900	122.100				
c-oh	400.10	1.351	c3-c-o	67.400	123.200				
c-c3	313.00	1.524	c-oh-ho	49.900	106.550				
ho-oh	371.40	0.973	c-c3-hc	46.900	108.770				
c3-hc	330.60	1.097	c-c3-c3	63.300	111.040				
c3-c3	300.90	1.538	c3-c-oh	68.400	112.730				
c3-oh	316.70	1.423	c3-c3-hc	46.300	109.800				
c3-h1	330.60	1.097	c3-c3-c3	62.900	111.510				
			hc-c3-hc	39.400	107.580				
			c3-c3-oh	67.500	110.190				
			c3-c3-h1	46.400	109.560				
			c3-oh-ho	47.400	107.260				
			h1-c3-oh	50.900	110.260				
DIHEDRAL			DIHEDRAL						
o-c-oh-ho	1	2.300	180.000	-2.000	c3-c3-c3-c3	1	0.180	0.000	-3.000
o-c-oh-ho	1	1.900	0.000	1.000	c3-c3-c3-c3	1	0.250	180.000	-2.000
o-c-c3-hc	1	0.800	0.000	-1.000	c3-c3-c3-c3	1	0.200	180.000	1.000
o-c-c3-hc	1	0.000	0.000	-2.000	hc-c3-c3-hc	1	0.150	0.000	3.000

o -c -c3-hc	1	0.080	180.000	3.000	c3-c3-c3-oh	9	1.400	0.000	3.000
o -c -c3-c3	6	0.000	180.000	2.000	c3-c3-c3-h1	9	1.400	0.000	3.000
c -c3-c3-hc	9	1.400	0.000	3.000	c3-c3-oh-ho	1	0.160	0.000	-3.000
c -c3-c3-c3	9	1.400	0.000	3.000	c3-c3-oh-ho	1	0.250	0.000	1.000
oh-c -c3-hc	6	0.000	180.000	2.000	hc-c3-c3-oh	1	0.000	0.000	-3.000
IMPROPER					hc-c3-c3-oh	1	0.250	0.000	1.000
c3-o -c -oh	1.1	180.0	2.0	h1-c3-c3-hc	9	1.400	0.000	3.000	
				h1-c3-oh-ho	3	0.500	0.000	3.000	
				oh-c -c3-c3	6	0.000	180.000	2.000	
				c3-c -oh-ho	2	4.600	180.000	2.000	
				c3-c3-c3-hc	1	0.160	0.000	3.000	

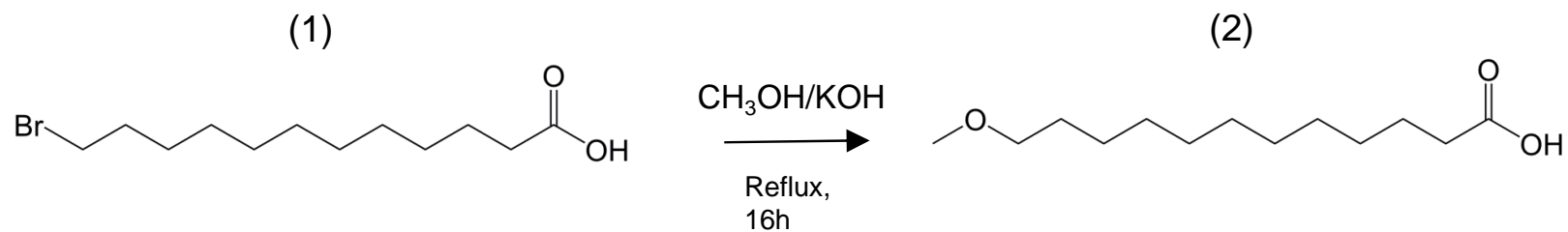
Table S7. Results of MD simulations. Measured the average distance between three carbons C12, C13, and C14 of myristic acid (MA) and oxygen of oxo ferryl cation radical complex ($+•\text{Heme-Fe}^{4+}=\text{O}$). Values were obtained based on 40,000 structures from 400 ns of NPT MD simulations at 303.15 K.

MA Carbons	AaeUPO		Fett	
	Avg. Distance	Distance in the highest population	Avg. Distance	Distance in the highest population
Fe=O...C14	4.11 ± 0.47 Å	3.80 ± 0.05 Å (3.9%)	4.28 ± 0.55 Å	4.40 ± 0.05 Å (4.1%)
Fe=O...C13	3.92 ± 0.44 Å	3.60 ± 0.05 Å (4.2%)	3.94 ± 0.41 Å	3.75 ± 0.05 Å (5.7%)
Fe=O...C12	3.96 ± 0.52 Å	3.65 ± 0.05 Å (4.9%)	4.40 ± 0.42 Å	4.55 ± 0.05 Å (6.1%)

Table S8. Reaction conditions for SCU-1 and SCU-2.

	SCU-1		SCU-2	
	START	END	START	END
Myristic acid _{initial} (mM)	100 (12g)		50 (4g)	
<i>t</i> -BuOH (%) v/v	20	10	20	20
KPi buffer pH 7.0 (mM)	80	38	80	45
Fett _{pic} mutant _{final} (μ M)	0.2	1.2 (11 aliquots)	0.2	4 (7 aliquots)
[H ₂ O ₂] _{final} (1 mM H ₂ O ₂ /h from 100 mM stock)	0	47	0	36
Final Volume (mL)	500	1060	350	630
Reaction conditions	30°C, 600 rpm, 164h reaction time		30°C, 600 rpm 96 h reaction time	

a



b

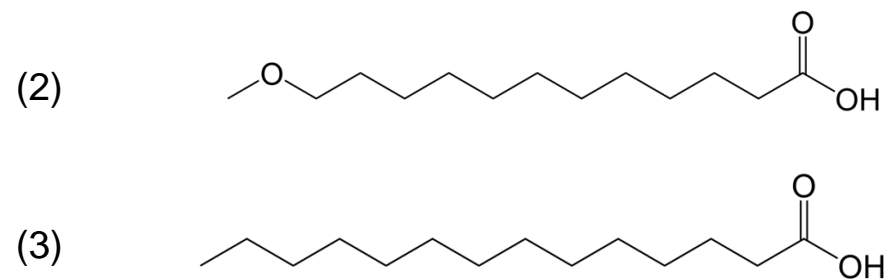


Figure S1. MLA synthesis and structural features. (a) Scheme for the synthesis of 12-bromododecanoic acid (1) into 12-methoxydodecanoic acid (12-methoxylauric acid, MLA) (2). (b) Structural comparison between (2) and tetradecanoic (myristic) acid (3).

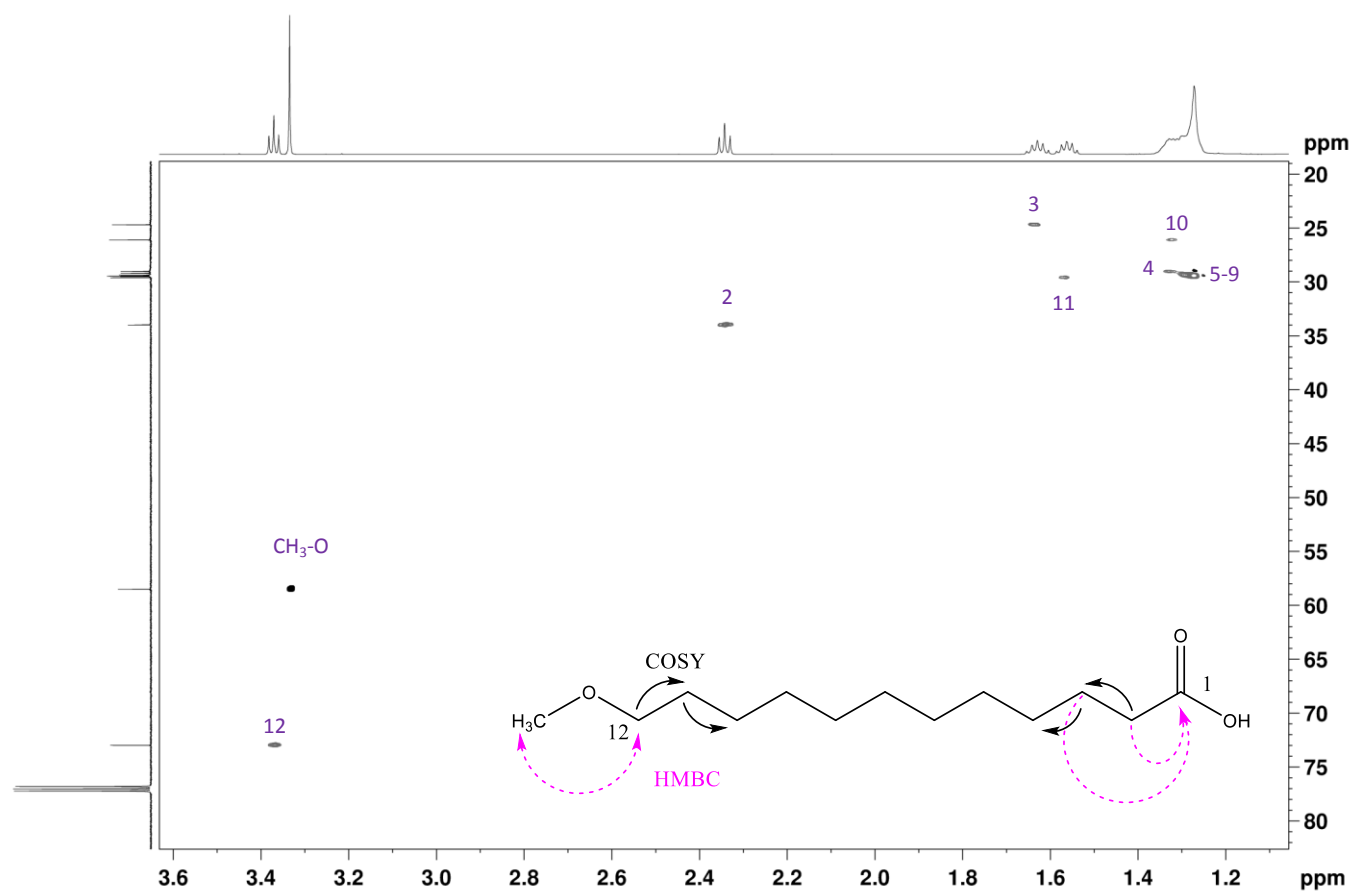
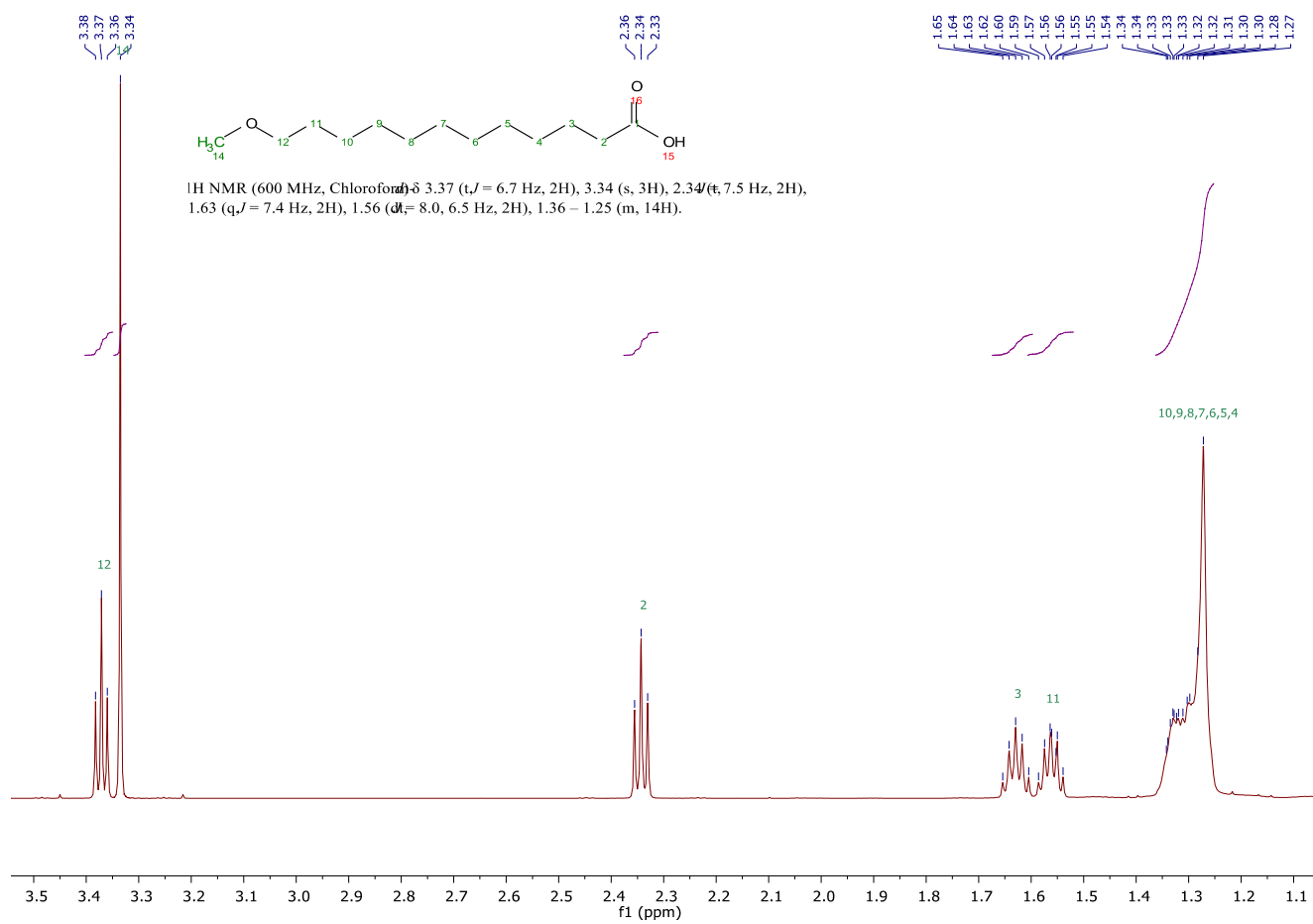


Figure S2. Determination of MLA by DEPT-HSQC with signal assignment. Observed correlations between homonuclear correlation COSY (black) and heteronuclear correlation HBMC (pink).

Figure S3. ¹H NMR of MLA.

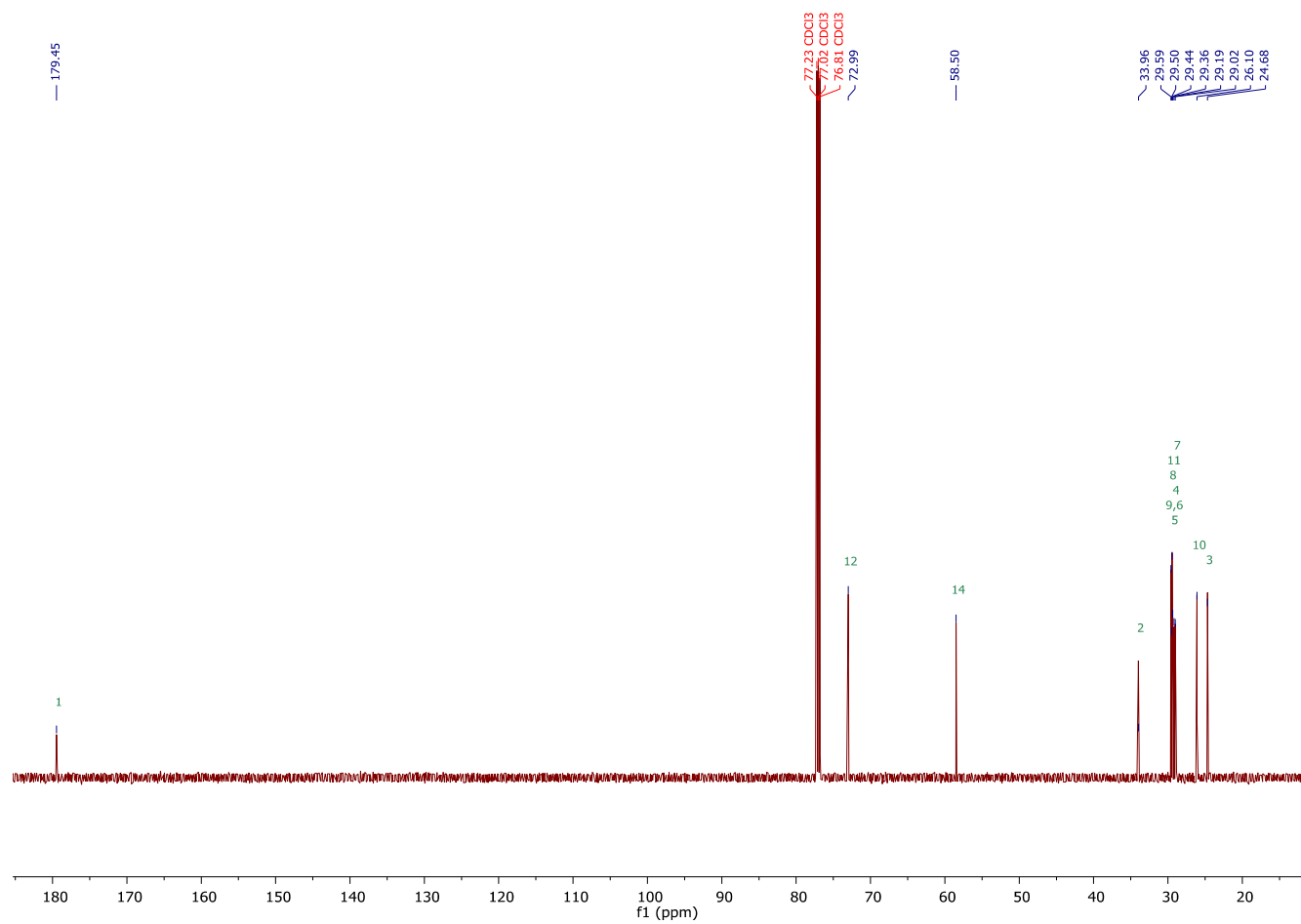


Figure S4. ¹³C NMR of MLA.

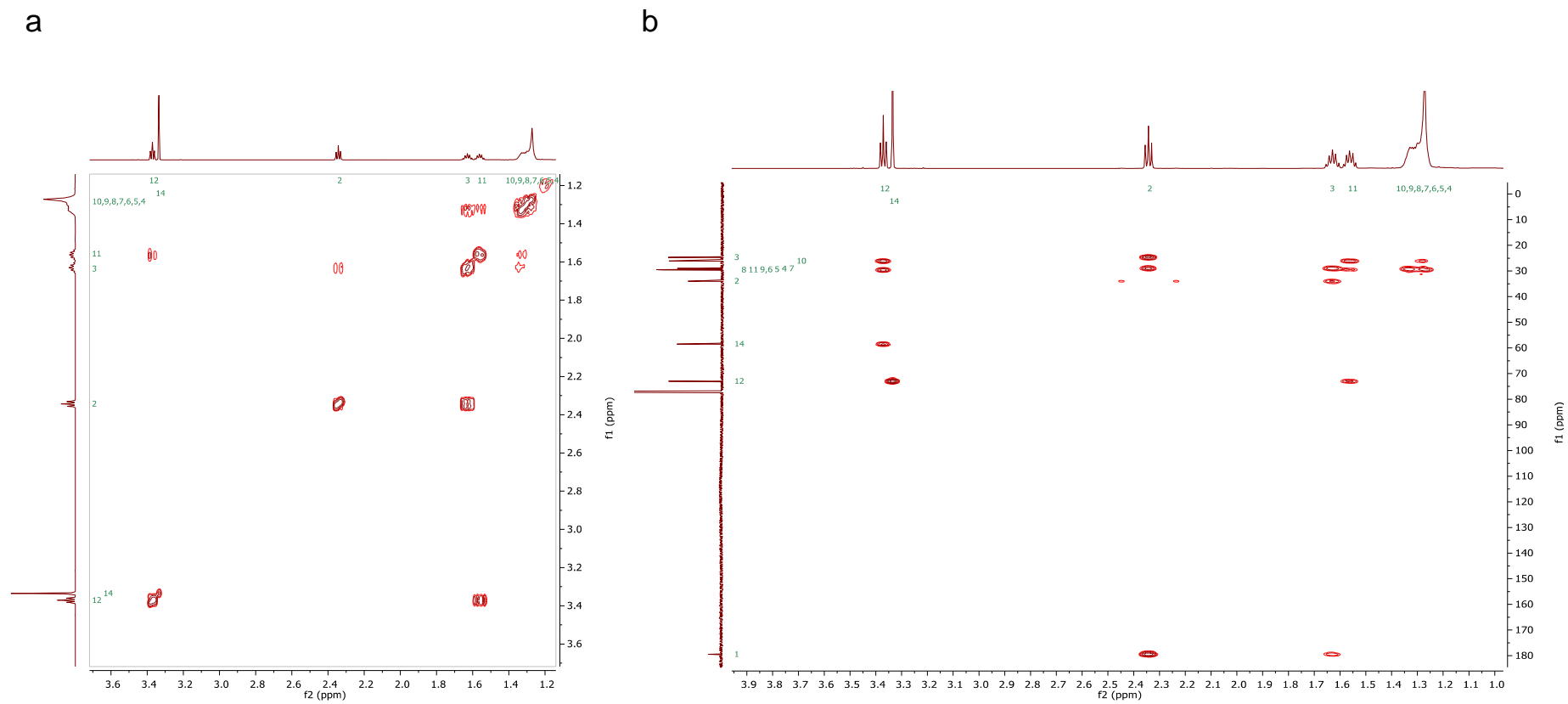


Figure S5. COSY (a) and HMBC (b) for MLA.

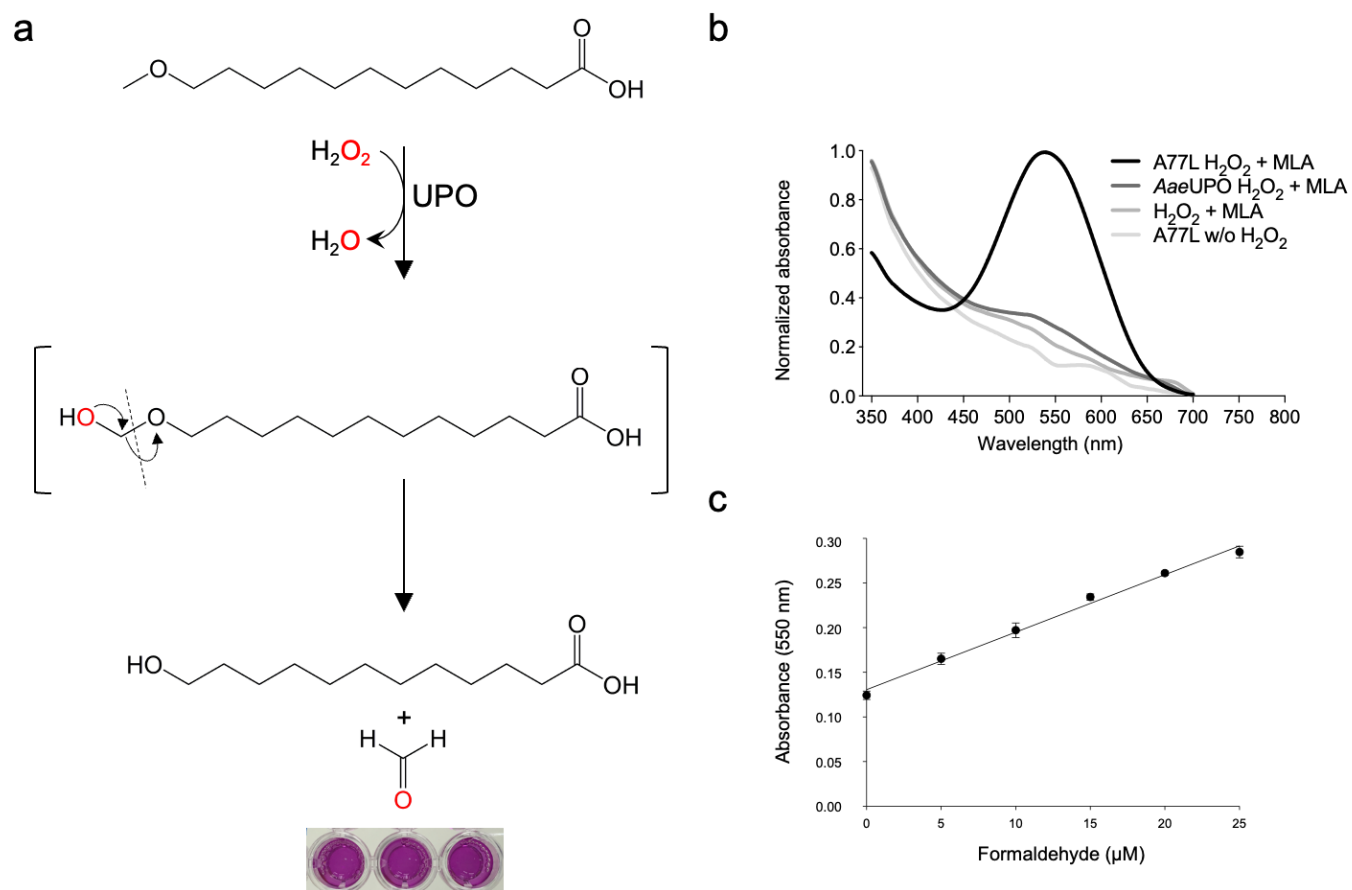


Figure S6. MLA screening assay. Hydroxylation of MLA at ω position by UPO releases formaldehyde, which forms a colored complex with purpald reagent (**a**). Spectrum of purpald-formaldehyde complex with its maximum of absorbance at 550 nm (**b**). To assess the linearity of the assay (**c**), 70 μL of supernatant together with 80 μL of reaction mixture containing 2 mM H_2O_2 in 100 mM potassium phosphate buffer pH 7.0, 12.5% (v/v) acetonitrile and different concentrations of formaldehyde were mixed with 50 μL of 100 mM Purpald dissolved in 2N NaOH. The reactions were shaken vigorously for 15 min. Thereafter, absorbance was monitored at 550 nm in a plate reader. Each point and standard deviation came from three independent measurements.

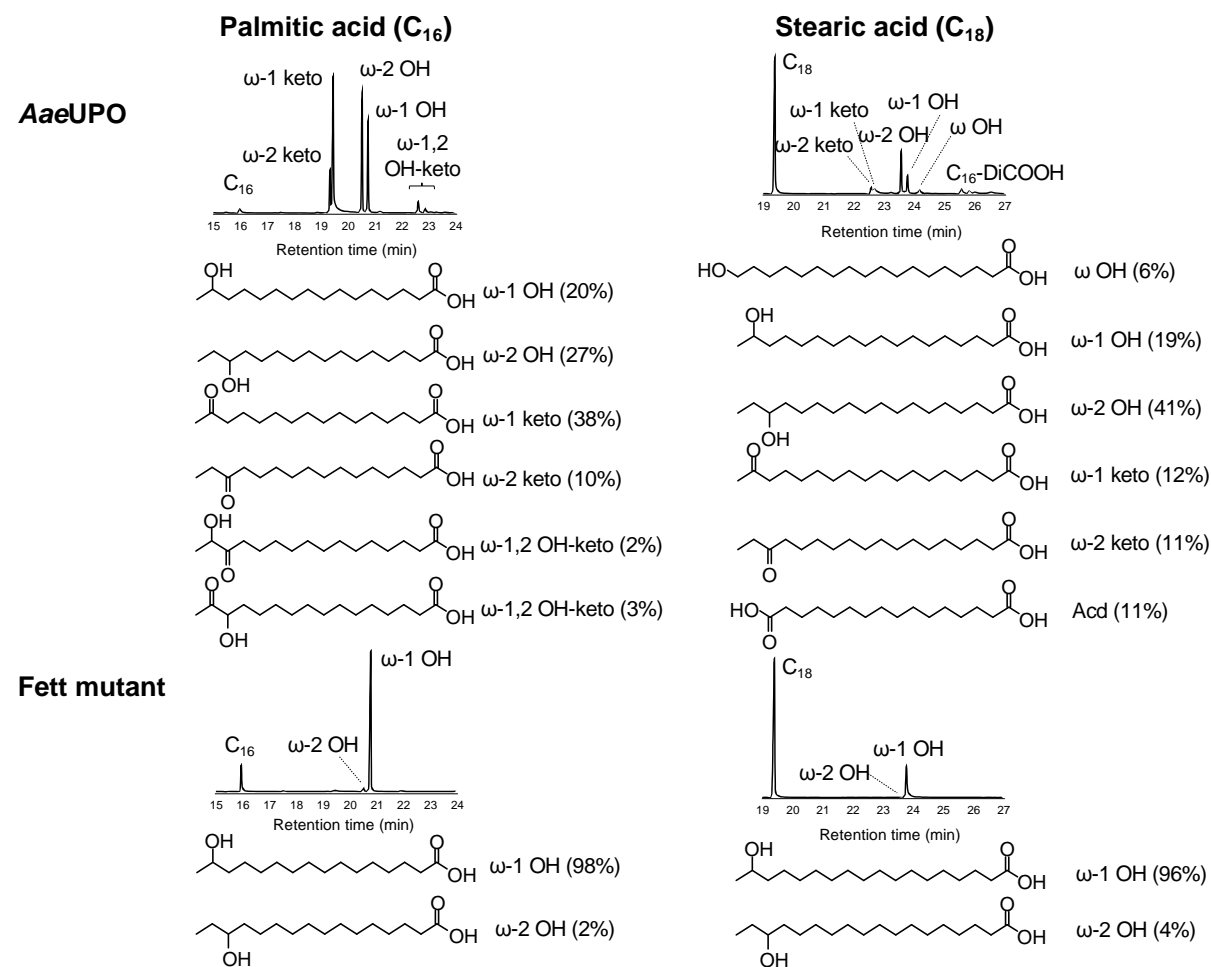


Figure S7. GC-MS analysis of the *AaeUPO* and *Fett* mutant reactions with palmitic acid (C₁₆) and stearic acid (C₁₈). The reactions were performed for 30 min at 30 °C and each reaction mixture contained 0.1 μM substrate, 2.5 mM H₂O₂, 0.1 μM purified enzyme and 20 % (v/v) acetone in potassium phosphate buffer 50 mM pH 7.0.

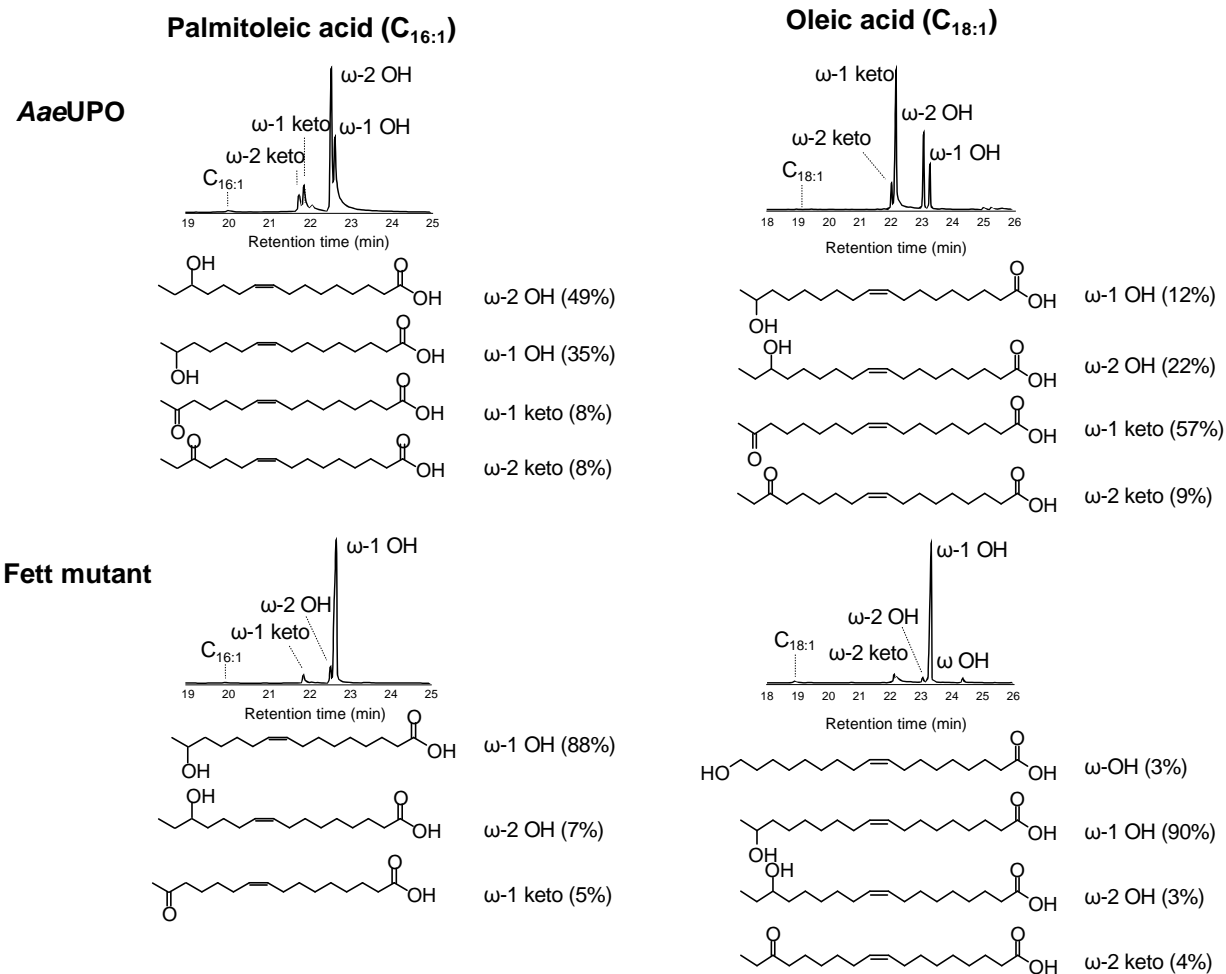


Figure S8. GC-MS analysis of the AaeUPO and Fett mutant reactions with palmitoleic acid (C_{16:1}) and oleic acid (C_{18:1}). The reactions were performed for 60 or 30 min at 30 °C and each reaction mixture contained 0.1 μM substrate, 2.5 mM H₂O₂, 0.1 μM purified enzyme and 20 % (v/v) acetone in potassium phosphate buffer 50 mM pH 7.0.

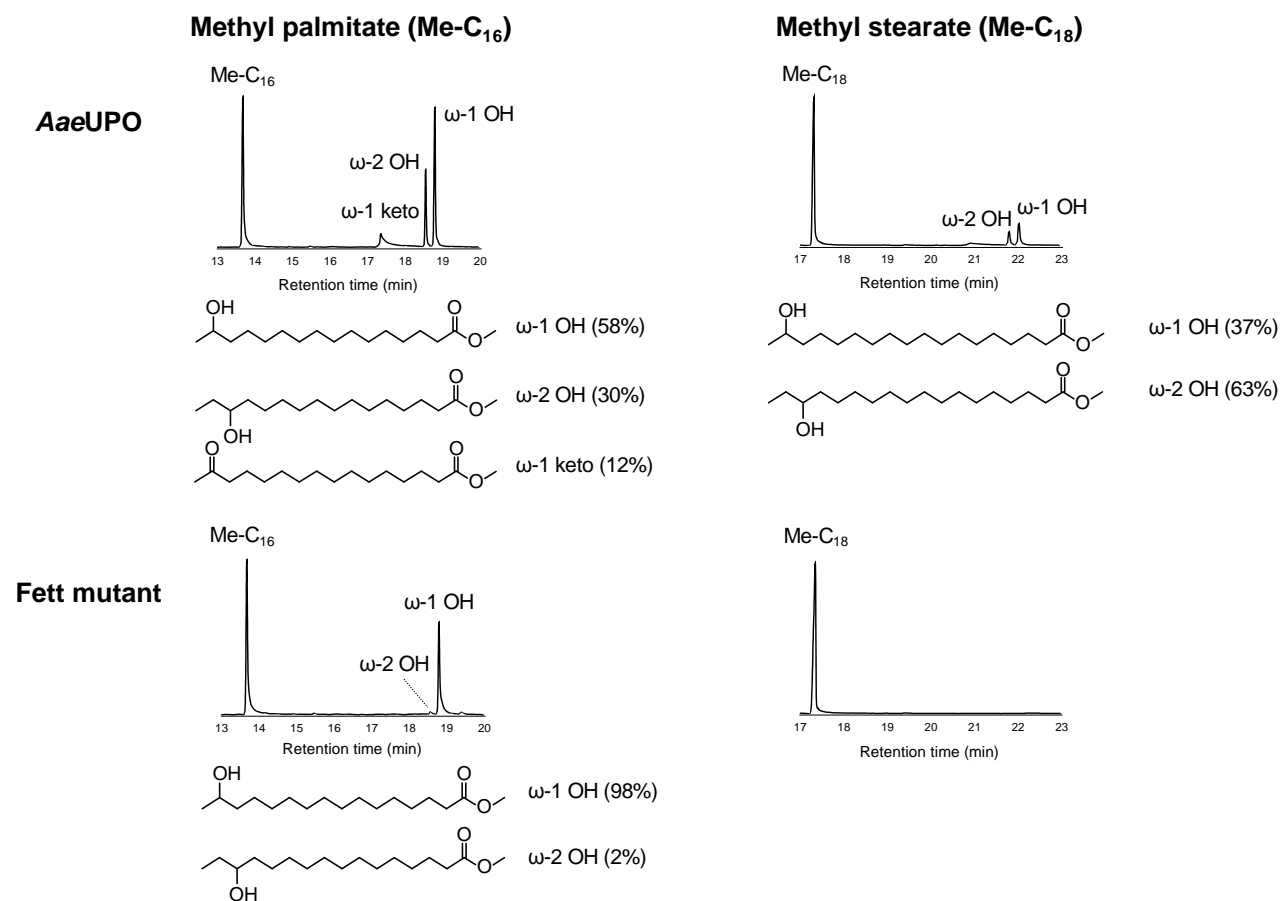


Figure S9. GC-MS analysis of the *AaeUPO* and *Fett* mutant reactions with methyl palmitate (Me-C₁₆) and methyl stearate (Me-C₁₈). The reactions were performed for 60 min at 30 °C and each reaction mixture contained 0.1 μM substrate, 2.5 mM H₂O₂, 0.5 μM purified enzyme and 40 % (v/v) acetone in potassium phosphate buffer 50 mM pH 7.0.

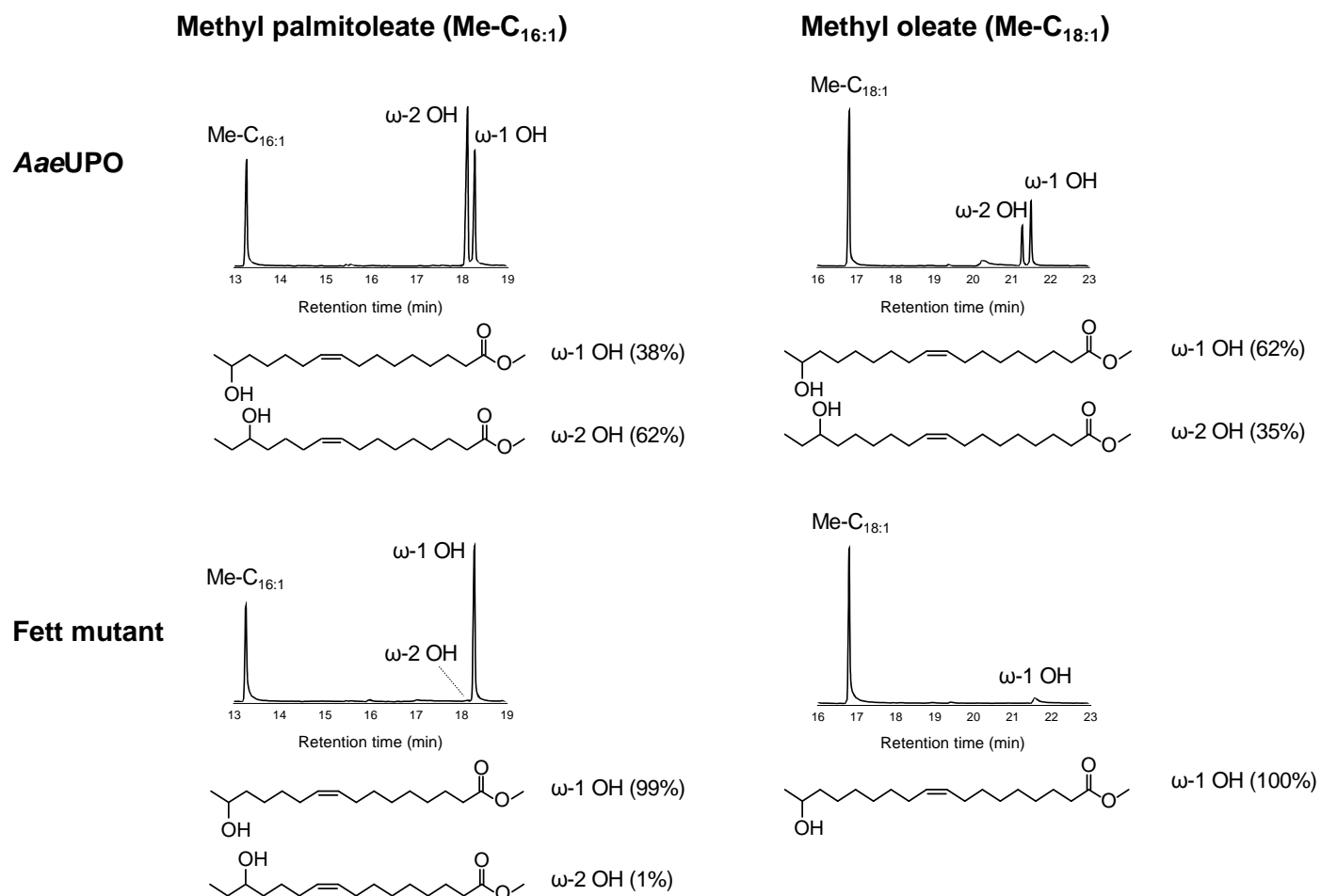


Figure S10. GC-MS analysis of the *AaeUPO* and *Fett* mutant reactions with methyl palmitoleate (Me-C_{16:1}) and methyl oleate (Me-C_{18:1}). The reactions were performed for 60 min at 30 °C and each reaction mixture contained 0.1 μM substrate, 2.5 mM H₂O₂, 0.5 μM purified enzyme and 40 % (v/v) acetone in potassium phosphate buffer 50 mM pH 7.0.

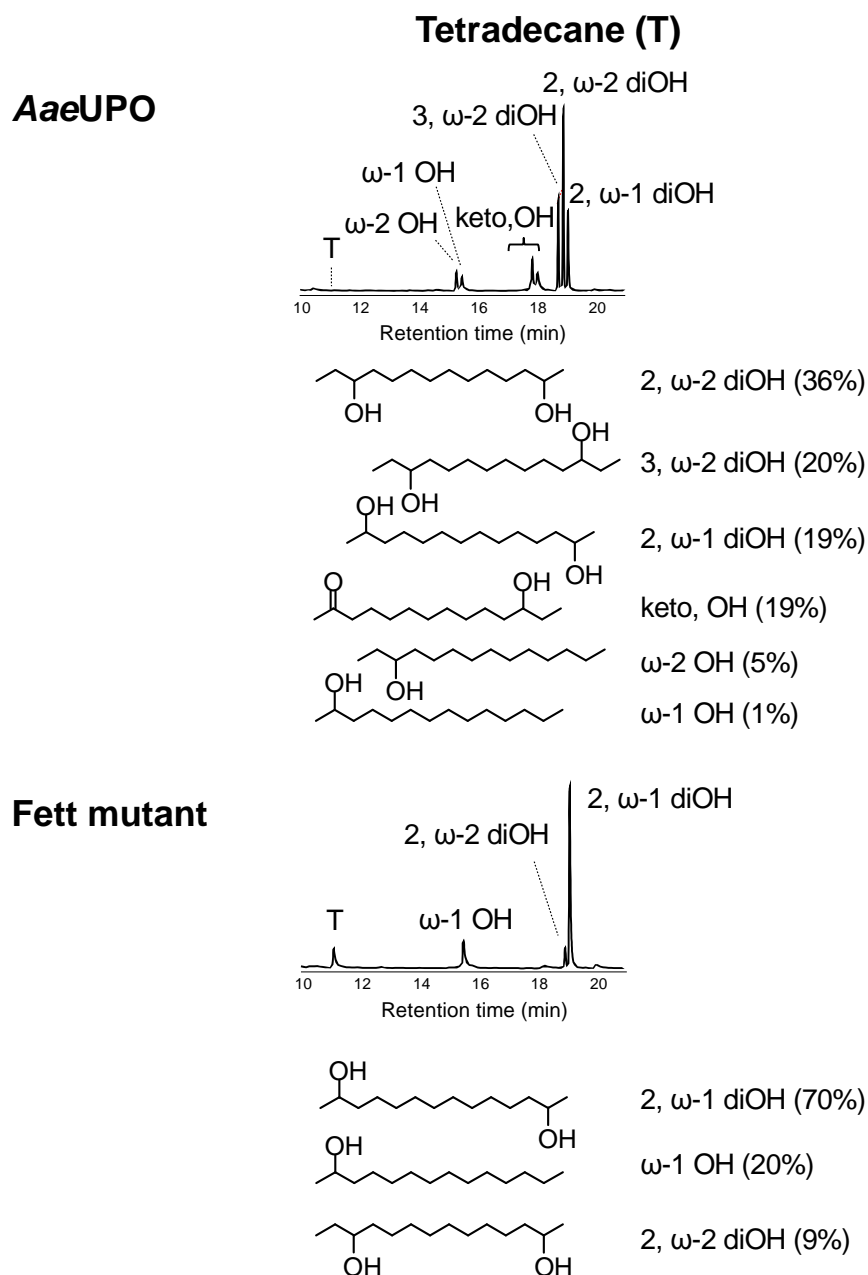


Figure S11. GC-MS analysis of the AaeUPO and Fett mutant reactions with tetradecane (T). The reactions were performed for 60 min at room temperature and each reaction mixture contained 0.1 μM substrate, 2.5 mM H₂O₂, 0.1 μM purified enzyme and 20 % (v/v) acetone in potassium phosphate buffer 50 mM pH 7.0.

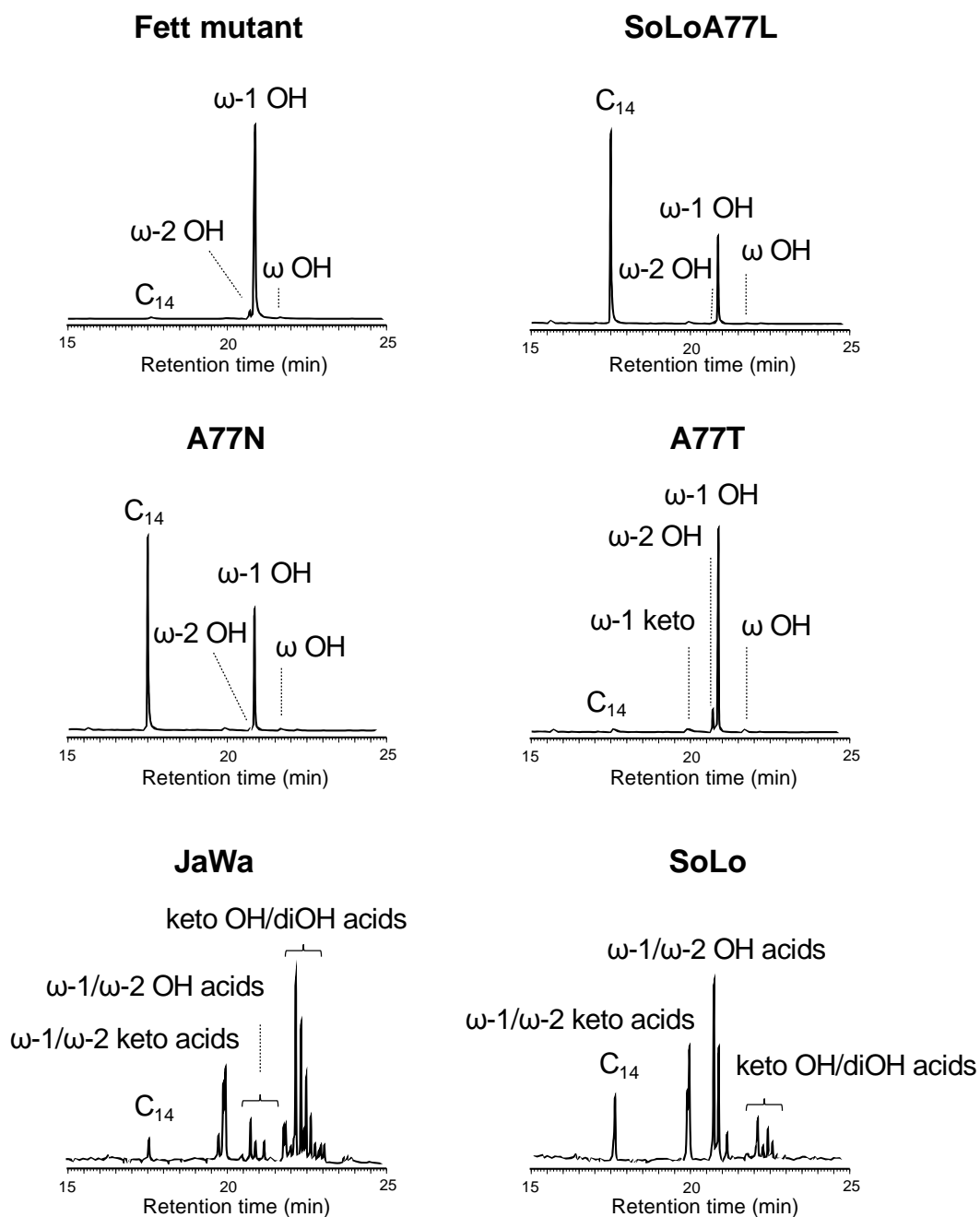


Figure S12. GC-MS analysis of enzymatic reactions with myristic acid (C_{14}). Reactions were performed for 30 min at 30°C containing 0.1 mM substrate (MA), 2.5 mM H_2O_2 , 0.1 μ M purified enzyme and 20 % (v/v) acetone in potassium phosphate buffer 100 mM pH 7.0. Reactions with higher amount of enzyme and peroxide (5 mM H_2O_2 , 0.5 μ M purified enzyme, 60 min) were tested with the less active A77N and SoLoA77L mutants.

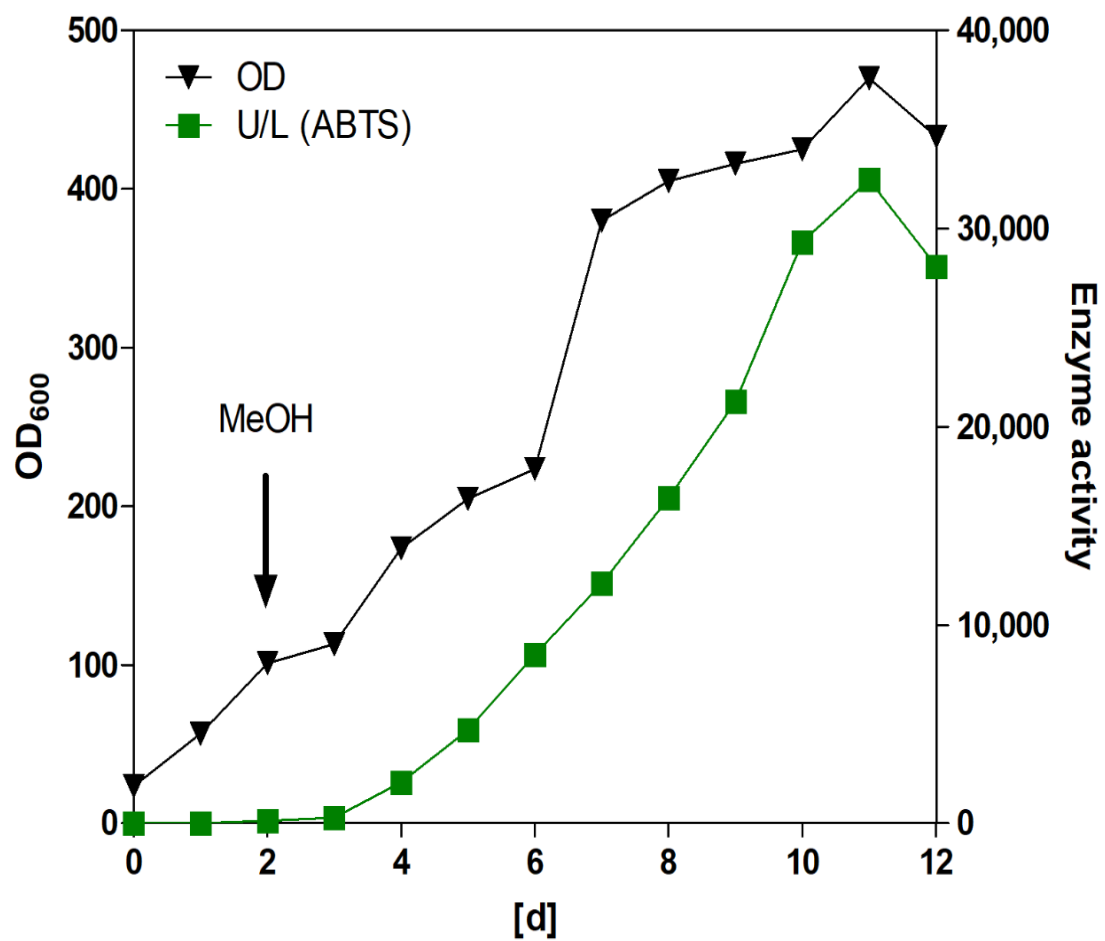


Figure S13. Time course of Fett secretion in a 12-L fed-batch reactor. The maximum UPO activity of 32000 U/L (based on ABTS oxidation) was reached after 11 days [d] (corresponding to 380 mg protein per liter).

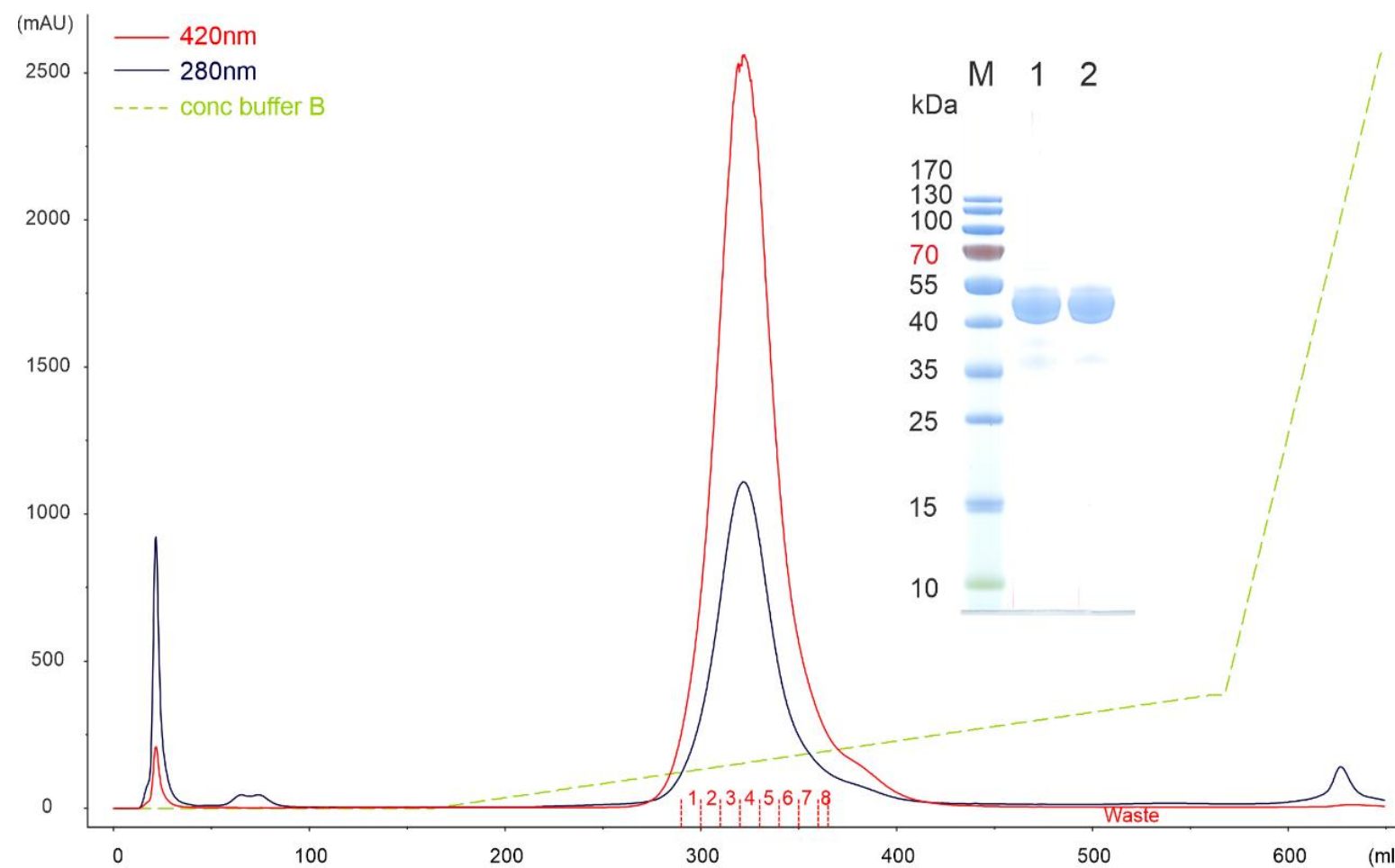


Figure S14. FPLC elution profile of the final Fett purification step (Q-Sepharose). Inset: SDS-PAGE of purified Fett_{pic} mutant after HIC (lane 1 - 10 µg) and after HIC/IEC (lane 2 - 10 µg), M – mass standards.

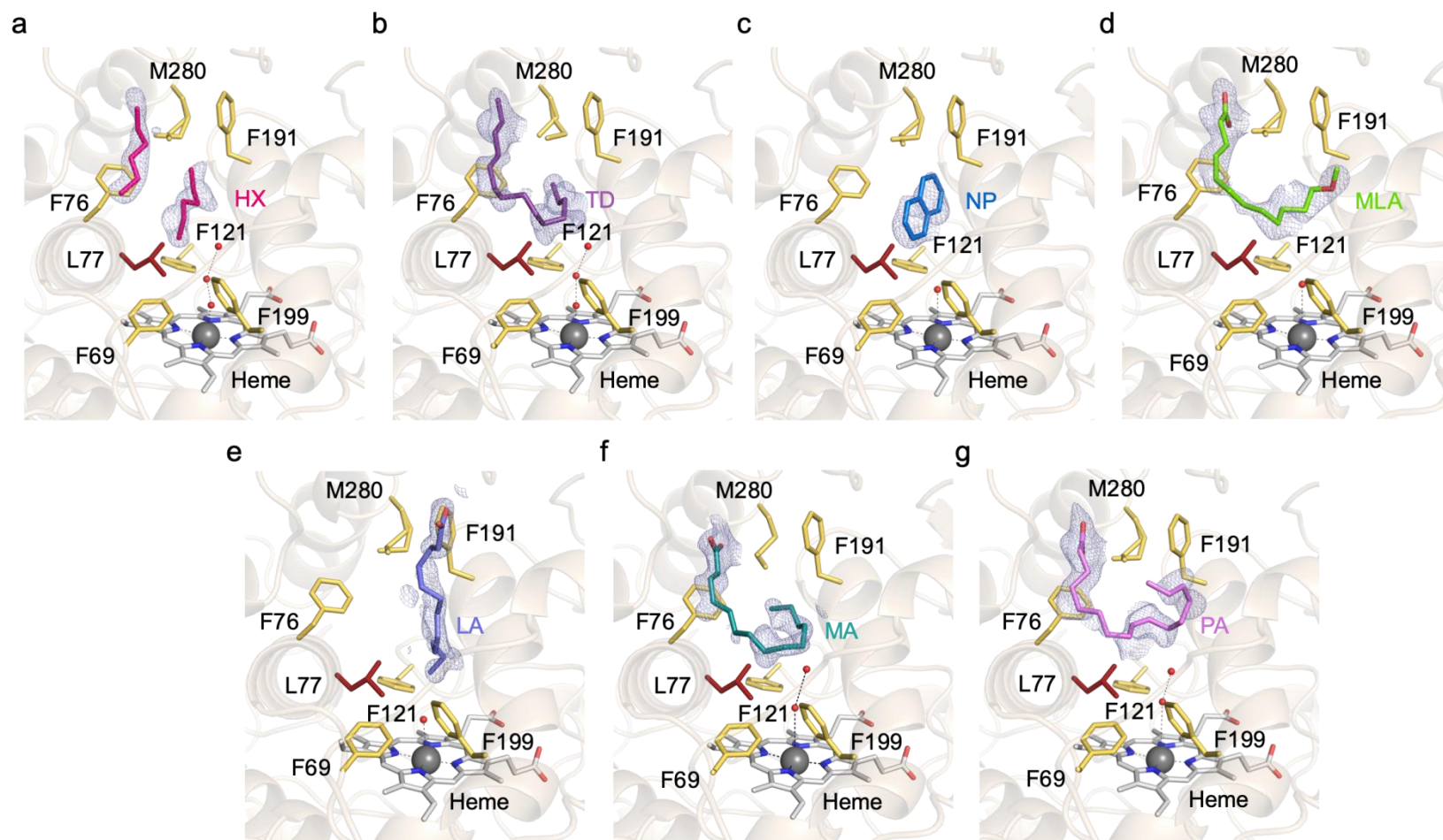


Figure S15. Crystal structures of *Fett* mutant in complex with different substrates. *Fett_{pic}* complexes with (a) hexane (HX), (b) tetradecane (TD), (c) naphthalene (NP), (d) MLA, (e) lauric acid (LA), (f) myristic acid (MA), and (g) palmitoleic acid (PA). Key residues for binding are represented as sticks and water molecules as red-spheres. The A77L mutation has been highlighted. 2Fo-Fc electron density at the ligands has been contoured at 0.8-1.0 σ . See also **Table S3**.

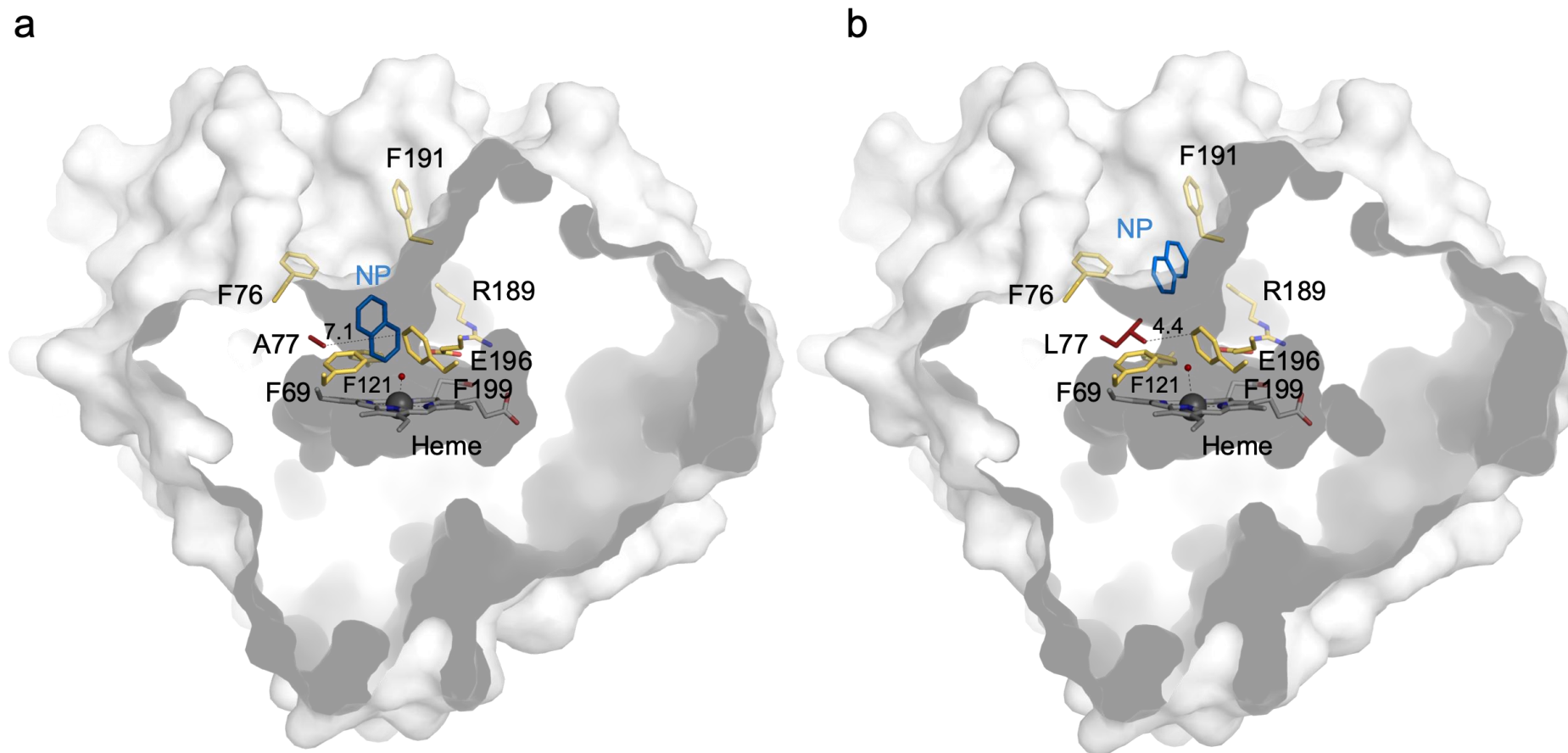


Figure S16. The constriction in the heme channel due to the A77L mutation. The parental AaeUPO (a) and the Fett_{pic} variant (b) complexed to naphthalene (NP) are represented in a sliced surface. The heme group, the Phe tripod (Phe69, Phe121, Phe199), the acid-base pair (Arg189, Glu196) and the Phe residues limiting the access to the channel (Phe76, Phe191) together with A77L mutation are highlighted. See also **Table S3**.

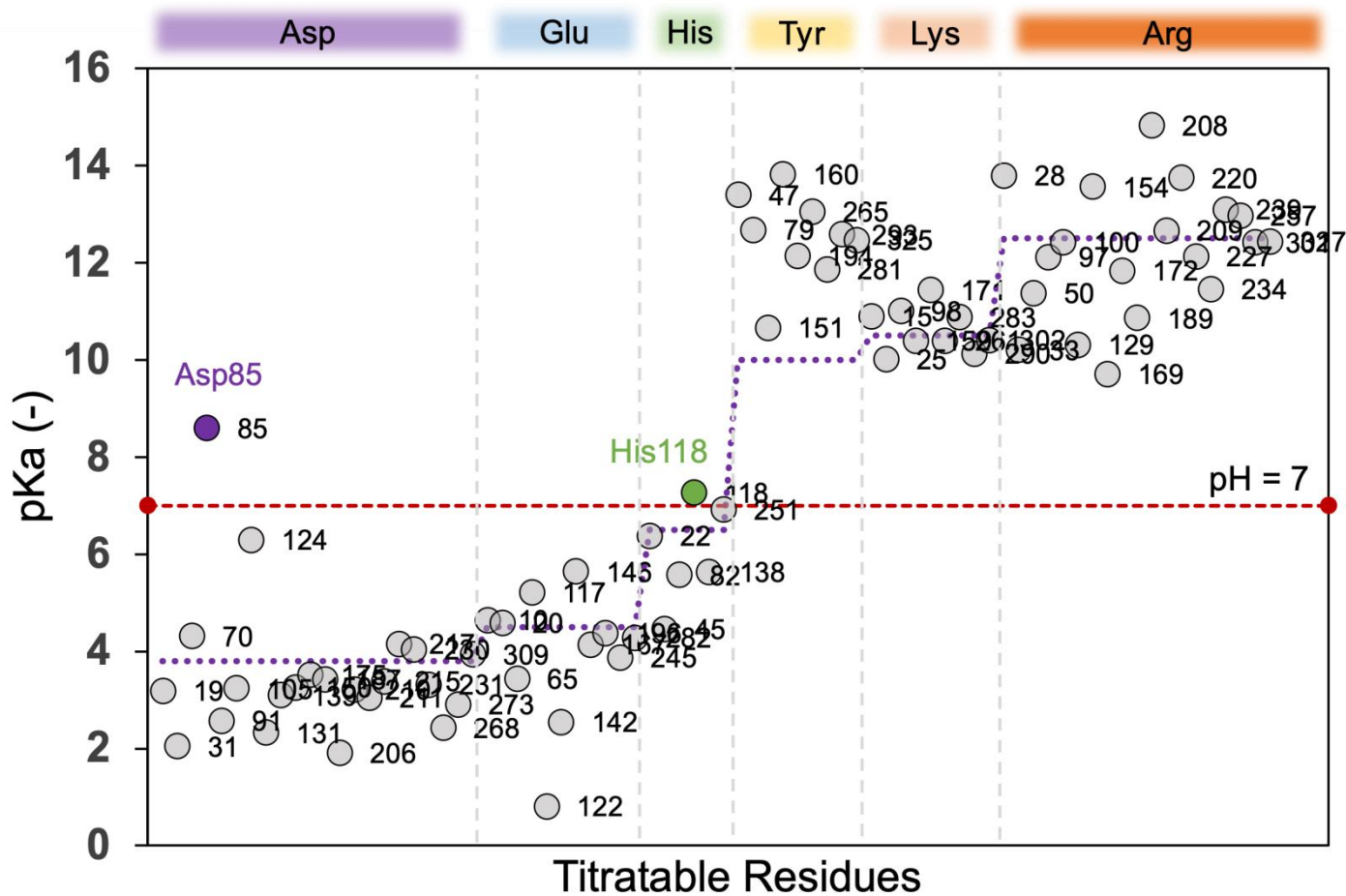


Figure S17. Determined pKa values for titratable residues present in AaeUPO.

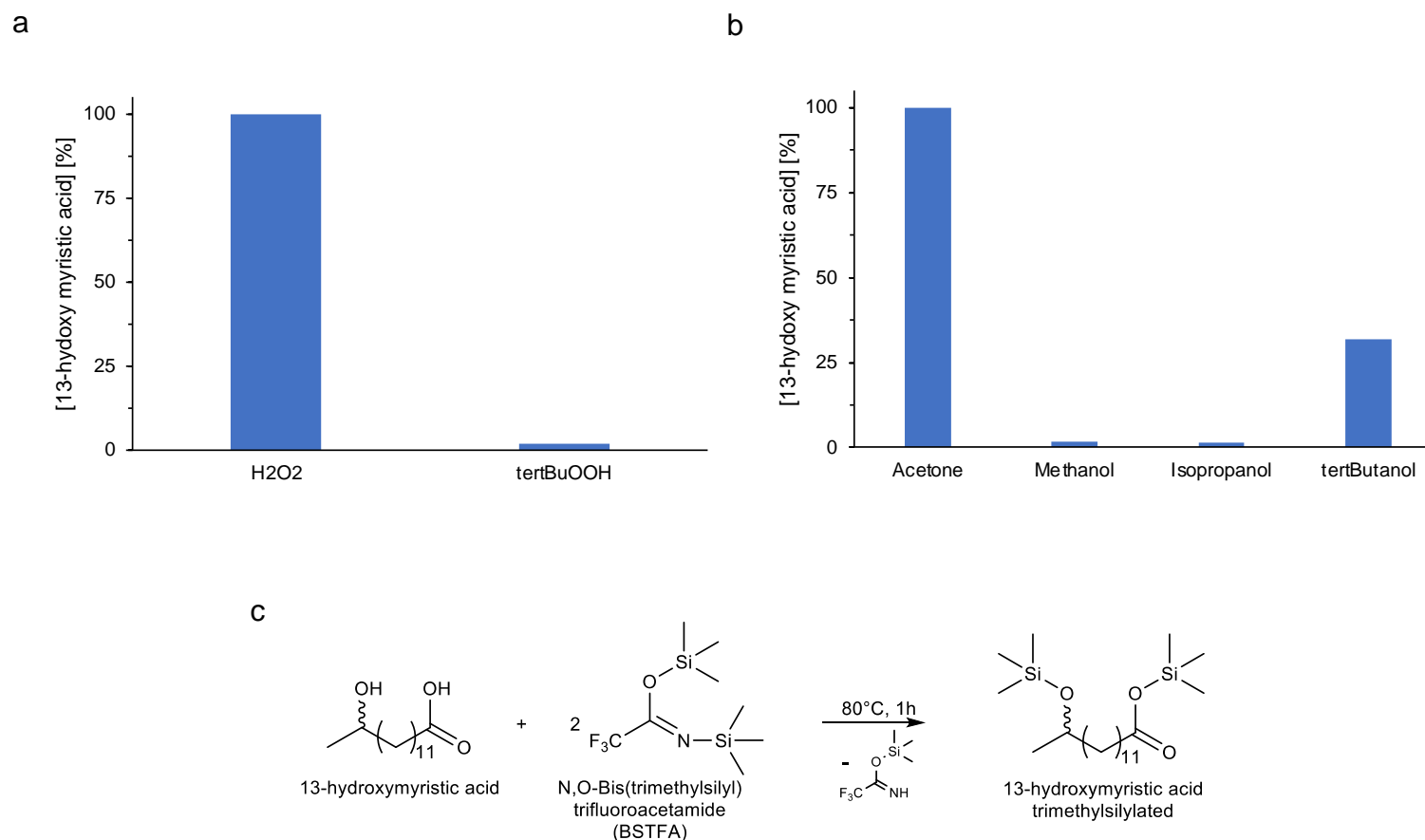
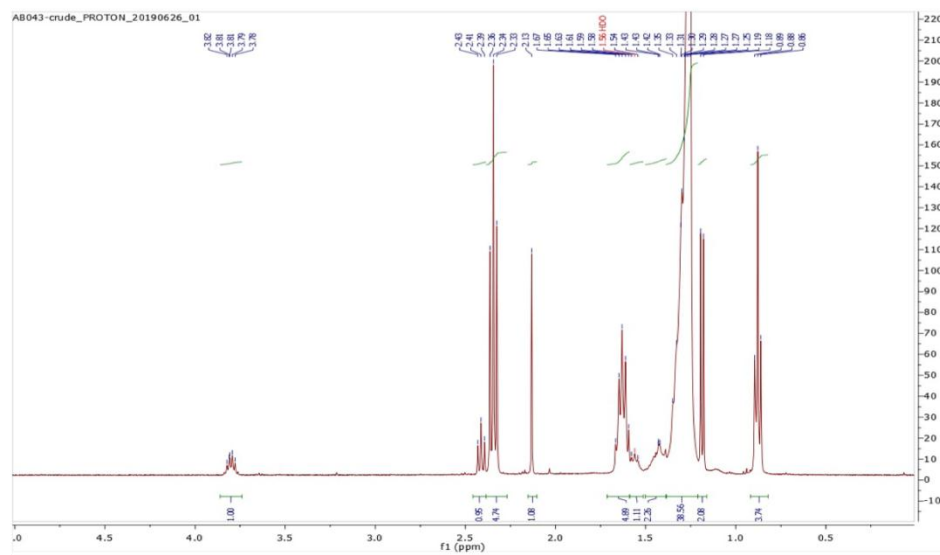


Figure S18. Benchmarking of different hydroperoxides (a) and organic cosolvents (b) for the preparative synthesis of ω -1 hydroxy-myristic acid. (a) hydroperoxides screening: Reactions were carried for 5 h at 30°C and 500 rpm in 80 mM potassium phosphate buffer pH 6.0 containing 5 mM myristic acid, 200 nM purified *Fett_{pic}* mutant and 20% (v/v) acetone. Reactions were fed with a constant supply of 1 mM/h of different peroxides by a syringe pump system from a 120 mM stock solution. (b) Organic cosolvent screening: Reactions were carried for 5 h at 30°C and 500 rpm in 80 mM potassium phosphate buffer pH 6.0 containing 5 mM myristic acid, 200 nM purified *Fett_{pic}* mutant and 20% (v/v) of different cosolvents. Reactions were fed with a constant supply of 1 mM/h of H₂O₂ by a syringe pump system from a 120 mM stock solution. (c) For both screenings, extraction was performed in methyl-tert-butylether (MTBE) and derivatisation with BSTFA and analyzed by GC/FID.

a



b

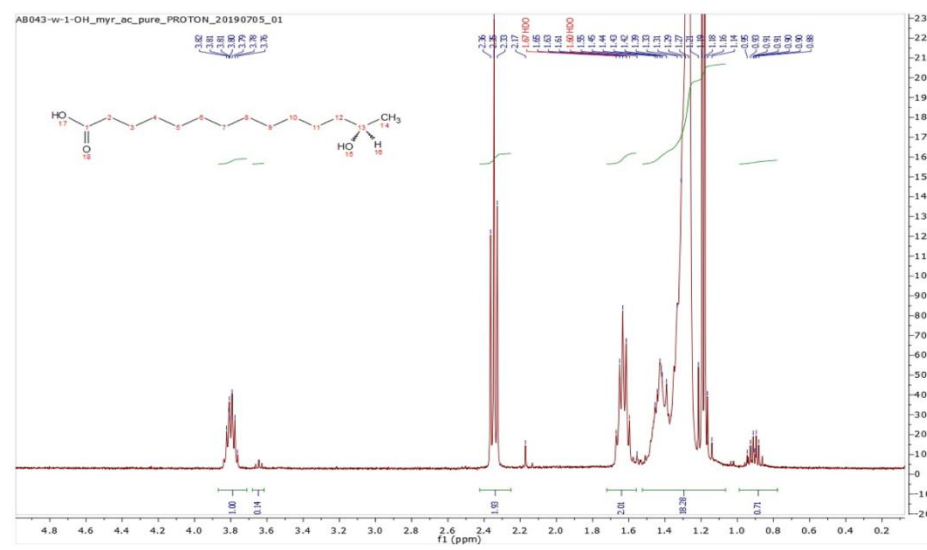
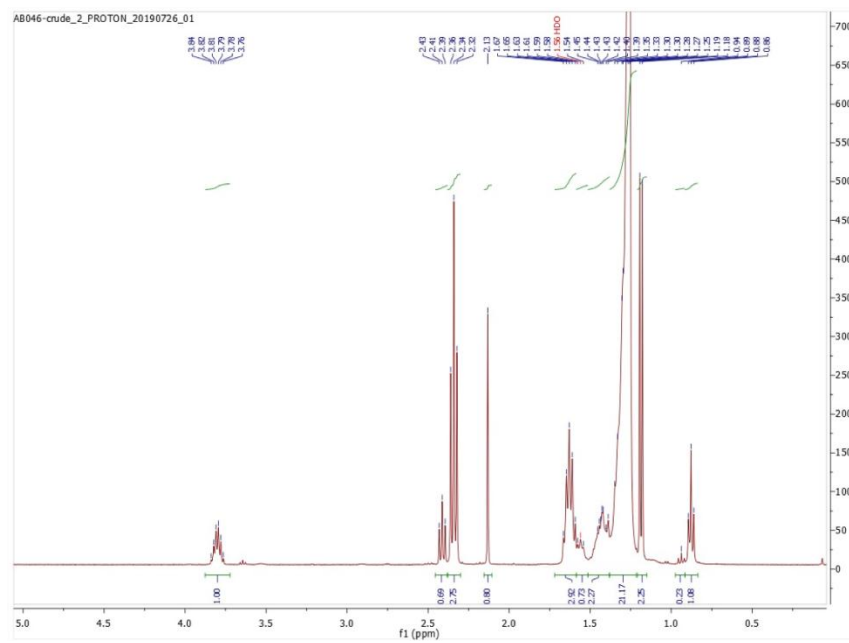


Figure S19. ¹H NMR of SCU-1. (a) Crude product mixture as isolated from the reaction and (b) after flash chromatographic purification.

a



b

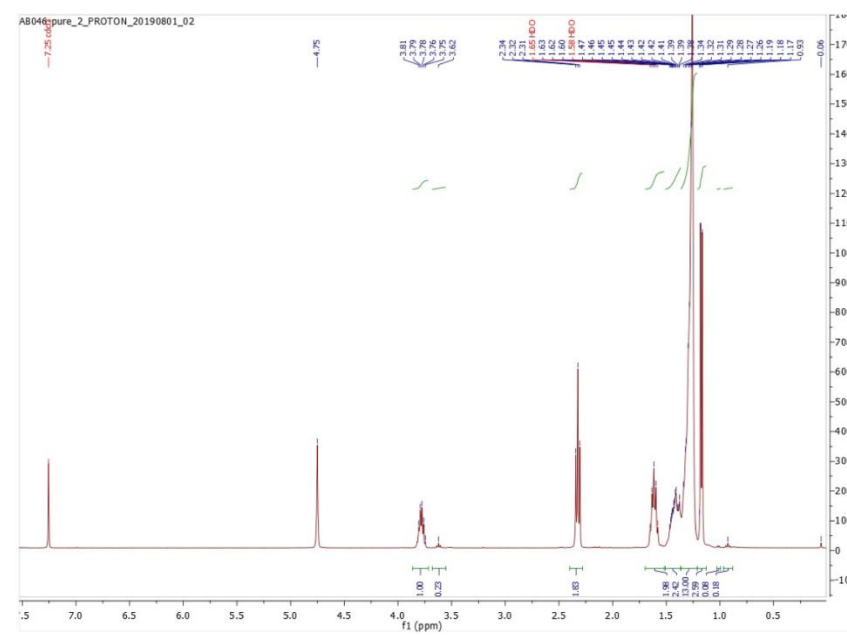


Figure S20. ¹H NMR of SCU-2. (a) Crude product mixture as isolated from the reaction and (b) after flash chromatographic purification.

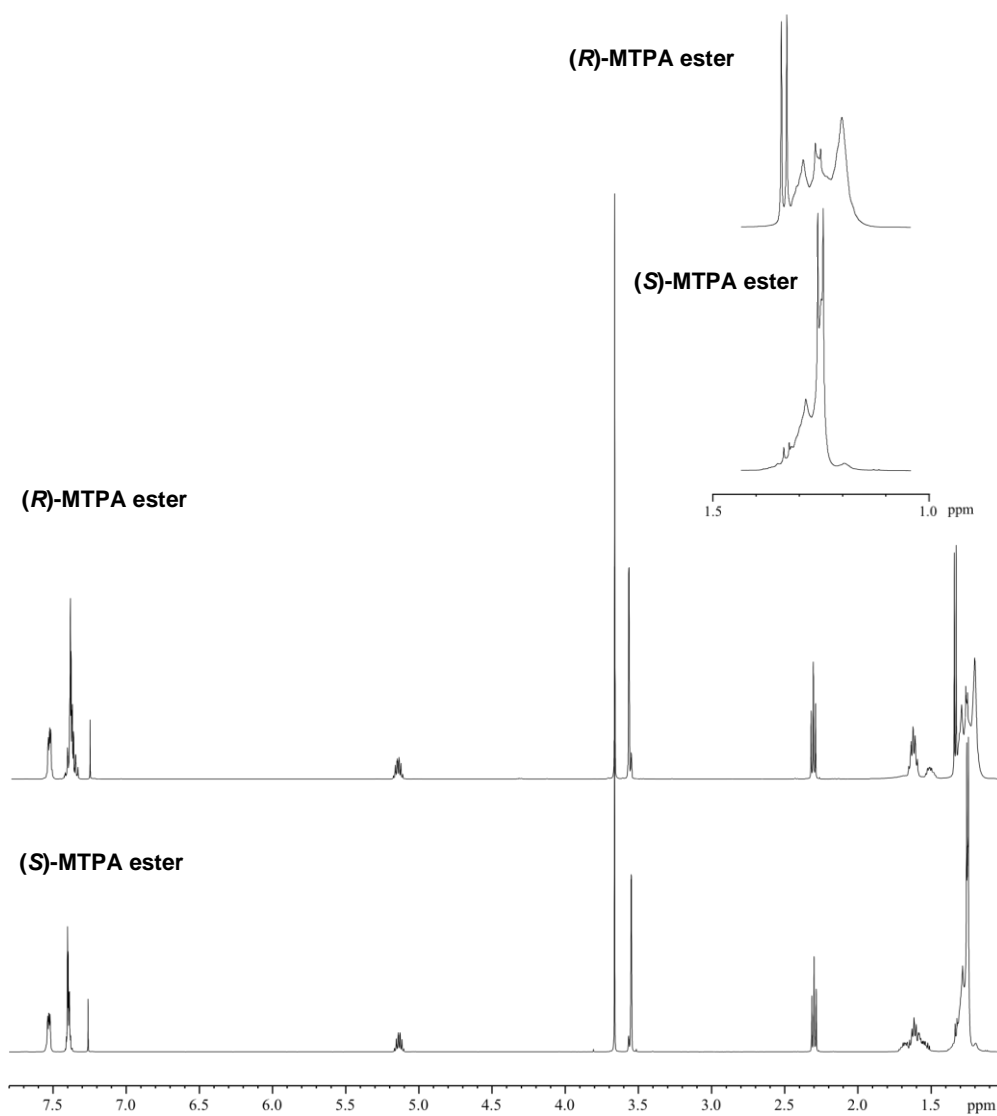


Figure S21. $^1\text{H-NMR}$ of methyl MTPA-13-hydroxymyristate. Reactions performed with (*R*)-MTPA-Cl (bottom) and (*S*)-MTPA-Cl (top).

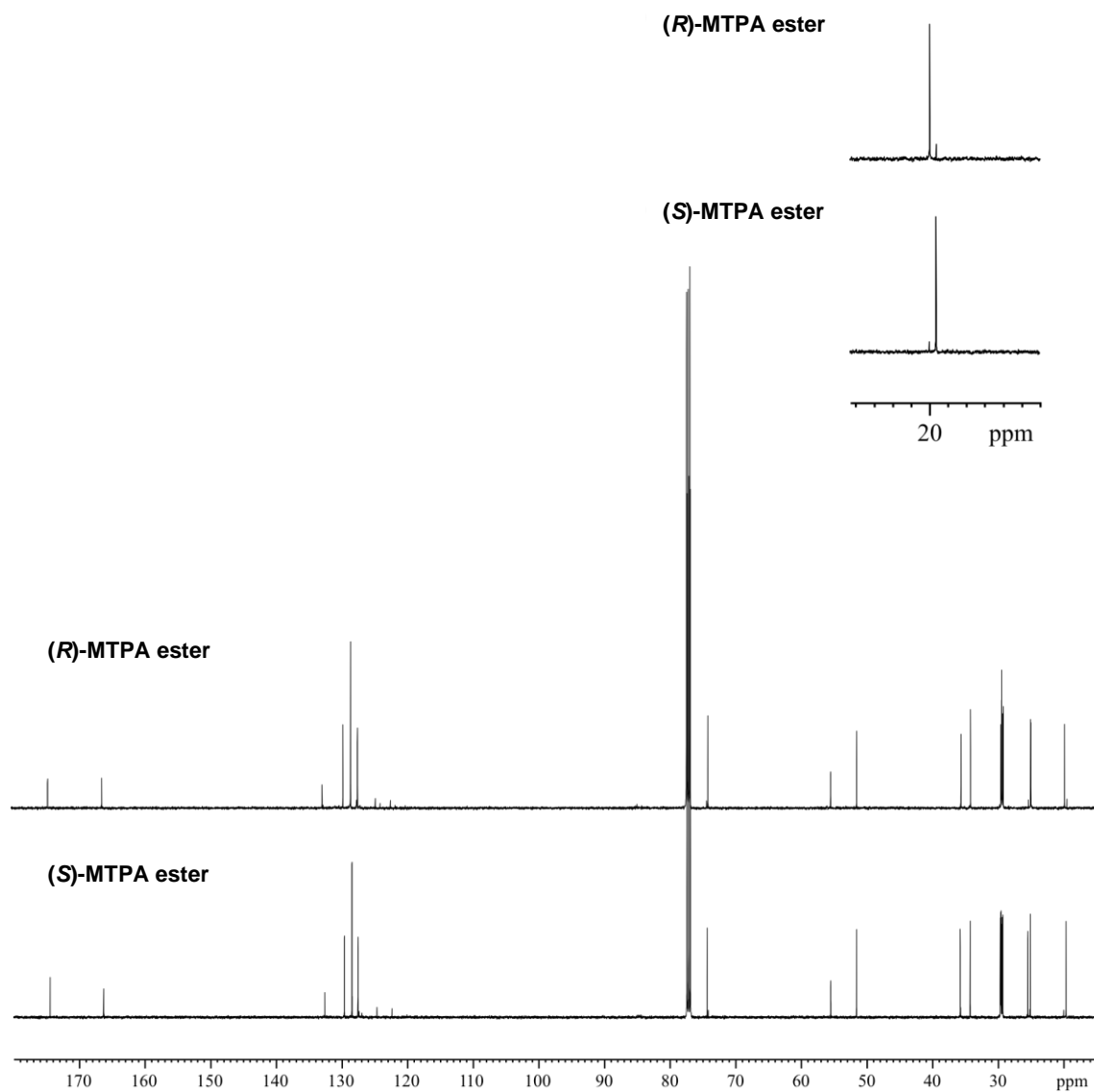


Figure S22. ^{13}C -NMR of methyl MTPA-13-hydroxymyristate. Reactions performed with (R)-MTPA-Cl (bottom) and (S)-MTPA-Cl (top).

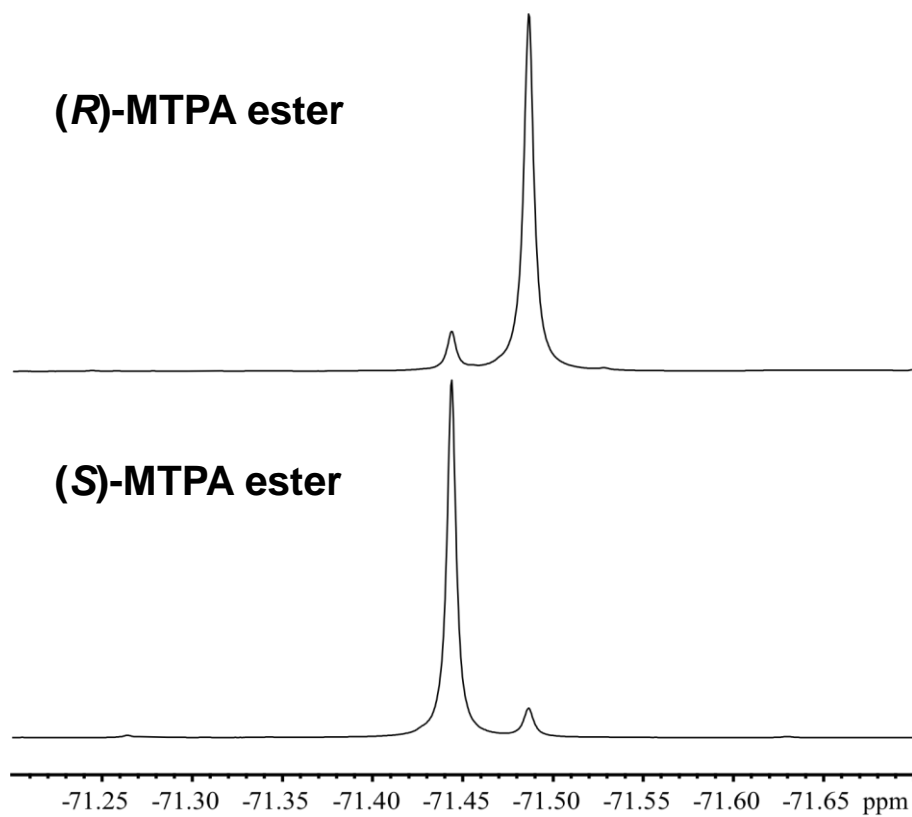


Figure S23. ^{19}F -NMR of methyl MTPA-13-hydroxymyristate. Reactions performed with (*R*)-MTPA-Cl (bottom) and (*S*)-MTPA-Cl (top).